




## Oscillator strengths for $^2P - ^2S$ transitions in neutral boron


Saeed Nasiri <sup>1,\*</sup>, Sergiy Bubin <sup>1,†</sup> and Ludwik Adamowicz <sup>2,3,4,‡</sup>

<sup>1</sup>*Department of Physics, Nazarbayev University, Astana 010000, Kazakhstan*

<sup>2</sup>*Department of Chemistry and Biochemistry, University of Arizona, Tucson, Arizona 85721, USA*

<sup>3</sup>*Department of Physics, University of Arizona, Tucson, Arizona 85721, USA*

<sup>4</sup>*Centre for Advanced Study (CAS), the Norwegian Academy of Science and Letters, N-0271 Oslo, Norway*

 (Received 21 October 2023; revised 12 February 2024; accepted 29 February 2024; published 11 April 2024)

In this study, we perform a set of benchmark variational calculations for the ground state and for the 18 lowest bound excited  $^2S$  and  $^2P$  states of the boron atom. The nonrelativistic wave function of each state is generated in an independent calculation by expanding its wave function in terms of a large number (10 000–16 000) of all-electron explicitly correlated Gaussian functions (ECG). The Hamiltonian used in the calculations explicitly depends on the mass of the boron nucleus. The nonlinear parameters of the ECGs are extensively optimized with a procedure that employs the analytic energy gradient determined with respect to these parameters. These highly accurate nonrelativistic wave functions are used to compute the transition dipole moments and the corresponding oscillator strengths for all allowed transitions between the considered states. These quantities are reported for the transitions of the  $^{10}\text{B}$  and  $^{11}\text{B}$  isotopes, as well as for the boron atom with an infinite nuclear mass,  $^\infty\text{B}$ , and used to evaluate the isotopic shifts of the oscillator strengths. The results generated in this work are considerably more accurate than the data obtained in the previous theoretical calculations.

DOI: [10.1103/PhysRevA.109.042813](https://doi.org/10.1103/PhysRevA.109.042813)

### I. INTRODUCTION

Quantum mechanics (QM) provides a powerful framework to perform highly accurate calculations regardless of system's size. There are two main obstacles in performing such calculations. The first one is related to the available basis functions which are used in expanding the wave function of the system. There are, in general, two types of basis functions used in atomic and molecular QM calculations, i.e., single-particle orbitals and explicitly correlated basis functions. The calculations performed with single-particle orbitals usually converge very slowly; for instance, millions of terms are required in CI calculations to reach a microhartree accuracy even for the ground state of the helium atom [1]. In contrast, if the basis functions explicitly depend on the interelectron distances, as it is the case for the explicitly correlated basis functions (ECBF), the calculations converge much faster in terms of the basis set size. Despite the usually high computational cost, the accuracy of the results obtained in the ECBF calculations is much higher than in the orbital calculations, particularly when the basis functions are optimized.

Two kinds of ECBF are most popular in atomic and molecular QM calculations, i.e., the Hylleraas-type functions (Hy) and the Gaussian-type functions (ECG). The Hy functions usually offer superior accuracy and allow to generate the most precise data for the smallest atomic and molecular systems such as the helium [2–7] and lithium atoms [8–13] and the  $\text{H}_2$  molecule [14–18]. However, the application of the Hy func-

tions in calculations of atoms and molecules with more than two–three electrons has been challenging due to difficulties in evaluating the Hamiltonian matrix elements (see, for example, the work on the beryllium atom [19,20]). Thus, in QM calculations for larger atomic and molecular systems, the only currently available ECBF option are the ECG basis functions, which, at least in principle, enable high-accuracy calculations of systems with an arbitrary number of electrons. For more detailed information about applications of ECGs, see extended reviews in Refs. [21,22]). However, a drawback of the ECG functions is that, unlike in the case of the Hy functions, their use in variational calculations does not allow to satisfy the Kato's cusp conditions concerning the behavior of the wave functions of Coulomb systems at interparticle coalescence points. Also, the ECG functions decay too rapidly at infinity. Even though these deficiencies can be effectively remediated by employing larger basis sets and by thoroughly optimizing the ECG nonlinear parameters, increasing the number of ECGs in highly accurate QM calculations has been often hindered by the availability of computational resources. This obstacle is a bottleneck in obtaining more accurate results. It should be noted that increasing the number of basis functions and extending the time spent on the optimization of their nonlinear parameters not only leads to an improved accuracy of the total energy and the corresponding wave function of the considered state of the system, but also improves the accuracy of other atomic or molecular properties that are being studied. Our recent works on the lithium atom [23,24], beryllium atom [25], boron atom [26,27], and the LiH species [28,29] can serve as examples of highly accurate ECG calculations of ground and excited states of small atoms and molecules.

The use of the ECG basis in the framework of the variational method provides a tool for good representation of the

\*saeed.nasiri@nu.edu.kz

†sergiy.bubin@nu.edu.kz

‡ludwik@arizona.edu

wave function not only for the ground but also for excited states of the system. However, more ECGs are usually needed to achieve similar accuracy in the calculations for higher states than for lower states. This is a reflection of the fact that the wave functions of excited states have more sophisticated structure. This higher complexity also increases the amount of computational resources needed to resolve all features of the excited-state wave functions. To speed up the optimization of nonlinear parameters, which is the most time-consuming part of the calculations, our in-house computer code for ECG calculations employs the analytical energy gradient determined with respect to the parameters. The availability of the analytic energy gradient, which can be evaluated at a cost that is comparable to the cost of a single-point energy evaluation (only a few times more expensive), notably reduces the amount of the computational work. This, in turn, enables to achieve very high accuracy of the results for both ground and excited states as exemplified by our recent mentioned works where transition energies, fine structure splittings, and oscillator strengths were calculated for all stable isotopes of helium [30], lithium [23,24], beryllium [25], and boron [26,27]. In this work, we employ a similar approach to calculate (or, for some states, improve) the nonrelativistic transition energies and the corresponding oscillator strengths for 18 lowest doublet  $S$  and  $P$  states for all stable isotopes of the boron atom.

It is worth noting that the most accurate experimental measurements are mainly available for gases composed of highly volatile elements. In general, creating gaseous samples with sufficient optical density can be quite challenging. For those difficult cases, theoretical calculations become a practical alternative to determining the spectra. As mentioned, computational methods, especially methods employing ECBFs, are sometimes capable of providing estimates of the observables with an accuracy that can match or exceed the accuracy of the experimental data. To the authors' knowledge, apart from our previous works [26,27,31], the ECGs have only been employed to perform calculations on the first  ${}^2P$ ,  ${}^2S$ , and  ${}^2D$  states of the boron atom by two other groups [32–34]. In those studies, the oscillator strengths have not been investigated. The calculations mainly concerned the total nonrelativistic energies, as well as the corrections due to the finite nuclear mass and relativistic and quantum electrodynamics effects.

This investigation of the boron atom involves nonrelativistic calculations of the total and transition energies, and the oscillator strengths for two stable boron isotopes,  ${}^{10}\text{B}$  and  ${}^{11}\text{B}$ , and for the boron atom with an infinite nuclear mass,  ${}^\infty\text{B}$ . The calculations are done for the lowest nine  ${}^2P$  states and lowest ten  ${}^2S$  states. In order to provide a quick characterization of the considered states, in Table I we show their dominant electronic configurations taken from [35,36]. Partly due to strong configuration mixing (especially between  ${}^2S$  configurations) obtaining highly accurate results can be challenging even for methods employing ECBFs.

## II. METHOD

### A. Nonrelativistic nuclear-mass-dependent Hamiltonian

In the present nonrelativistic variational calculations of atoms, where the nuclear mass may be either finite or in-

TABLE I. Admixture of the leading single-particle configurations in the wave functions of the states of the neutral boron atom studied in this work. The data (i.e., the configurations and the corresponding percentages) are taken from Refs. [35,36].

State	Leading config.	Percent	2nd config.	Percent
$2\ {}^2P$	$2s^2 2p\ ({}^2P^o)$	95%	$2s^2 2p^3\ ({}^2P^o)$	4%
$3\ {}^2P$	$2s^2 3p\ ({}^2P^o)$	91%	$2p^2\ ({}^1S) 3p\ ({}^2P^o)$	7%
$4\ {}^2P$	$2s^2 4p\ ({}^2P^o)$	92%	$2p^2\ ({}^1S) 4p\ ({}^2P^o)$	7%
$5\ {}^2P$	$2s^2 5p\ ({}^2P^o)$	92%	$2p^2\ ({}^1S) 5p\ ({}^2P^o)$	7%
$6\ {}^2P$	$2s^2 6p\ ({}^2P^o)$	92%	$2p^2\ ({}^1S) 6p\ ({}^2P^o)$	7%
$7\ {}^2P$	$2s^2 7p\ ({}^2P^o)$	92%	$2p^2\ ({}^1S) 7p\ ({}^2P^o)$	7%
$8\ {}^2P$	$2s^2 8p\ ({}^2P^o)$	92%	$2p^2\ ({}^1S) 8p\ ({}^2P^o)$	7%
$9\ {}^2P$	$2s^2 9p\ ({}^2P^o)$	92%	$2p^2\ ({}^1S) 9p\ ({}^2P^o)$	7%
$10\ {}^2P$	$2s^2 10p\ ({}^2P^o)$			
$3\ {}^2S$	$2s^2 3s\ ({}^2S)$	95%	$2p^2\ ({}^1S) 3s\ ({}^2S)$	5%
$4\ {}^2S$	$2s^2 4s\ ({}^2S)$	95%	$2p^2\ ({}^1S) 4s\ ({}^2S)$	5%
$5\ {}^2S$	$2s^2 5s\ ({}^2S)$	86%	$2p^2\ ({}^1S) 5s\ ({}^2S)$	5%
$6\ {}^2S$	$2s^2 6s\ ({}^2S)$	77%	$2s 2p^2\ ({}^2S)$	12%
$7\ {}^2S$	$2s 2p^2\ ({}^2S)$	35%	$2s^2 7s\ ({}^2S)$	31%
$8\ {}^2S$	$2s^2 7s\ ({}^2S)$	58%	$2s 2p^2\ ({}^2S)$	31%
$9\ {}^2S$	$2s^2 8s\ ({}^2S)$	83%	$2s 2p^2\ ({}^2S)$	31%
$10\ {}^2S$	$2s^2 9s\ ({}^2S)$	95%	$2p^2\ ({}^1S) 9s\ ({}^2S)$	5%
$11\ {}^2S$	$2s^2 10s\ ({}^2S)$			
$12\ {}^2S$	$2s^2 11s\ ({}^2S)$			

finite, is first necessary to separate out the translational motion of the system as a whole. The Hamiltonian is obtained by separating out the atom's center-of-mass motion from the nonrelativistic laboratory-frame Hamiltonian. This separation yields an "internal" Hamiltonian that is used in the calculations. The separation is rigorous and reduces the  $N$ -particle problem ( $N = 6$  for the boron atom consisting of five electrons and a nucleus) to an  $n$ -pseudoparticle problem ( $n = N - 1 = 5$ ) represented by the internal Hamiltonian expressed in terms of the internal Cartesian coordinates  $r_i$ 's. These internal coordinates are chosen to be the position vectors of the electrons with respect to the nucleus (which serves as a reference particle). The internal nonrelativistic Hamiltonian has the following form in atomic units:

$$\begin{aligned}
 H_{\text{nr}}^{\text{int}} = & -\frac{1}{2} \left( \sum_{i=1}^n \frac{1}{\mu_i} \nabla_{r_i}^2 + \sum_{i=1}^n \sum_{j \neq i}^n \frac{1}{m_0} \nabla_{r_i} \cdot \nabla_{r_j} \right) \\
 & + \sum_{i=1}^n \frac{q_0 q_i}{r_i} + \sum_{i=1}^n \sum_{j < i}^n \frac{q_i q_j}{r_{ij}}. \tag{1}
 \end{aligned}$$

Here  $q_0 = 5$  is charge of the nucleus,  $q_i = -1$  ( $i = 1 - 5$ ) are the electron charges,  $m_0$  is the nuclear mass ( $m_0 = 18\,247.468\,631\,92$  for  ${}^{10}\text{B}$  and  $m_0 = 200\,63.736\,943\,13$  for  ${}^{11}\text{B}$  [37]),  $\mu_i = m_0 m_i / (m_0 + m_i)$  is the reduced mass of electron  $i$  ( $m_i = 1$ ,  $i = 1 - 5$ ), and  $r_{ij} = |\mathbf{r}_j - \mathbf{r}_i|$  is the distance between electrons  $i$  and  $j$ . The prime symbol ( $\prime$ ) stands for the vector and matrix transpose.

The calculations involving the nonrelativistic Hamiltonian  $H_{\text{nr}}^{\text{int}}$  can be carried out for both finite and infinite masses of the B nucleus. They yield the nonrelativistic ground- and excited-state energies ( $E_{\text{nr}}$ ) and the corresponding wave functions. Both the energy and the wave function depend on the mass

of the nucleus. In this work we report both the finite-mass and infinite-mass results. It should be noted that Hamiltonian (1) can be conveniently written in a compact matrix form [21] as

$$H_{\text{nr}}^{\text{int}} = -\nabla_r' \mathbf{M} \nabla_r + \sum_{i=1}^n \frac{q_0 q_i}{r_i} + \sum_{i=1}^n \sum_{j<i}^n \frac{q_i q_j}{r_{ij}}, \quad (2)$$

where

$$\nabla_r = \begin{pmatrix} \nabla_{r_1} \\ \vdots \\ \nabla_{r_n} \end{pmatrix} \quad (3)$$

is a  $3n$ -component gradient vector and  $\mathbf{M} = M \otimes \mathbf{I}$  is the Kronecker product of an  $n \times n$  matrix  $M$  and  $3 \times 3$  identity matrix  $\mathbf{I}$ . Matrix  $M$  has diagonal elements equal to  $1/(2\mu_1), \dots, 1/(2\mu_5)$ , while all off-diagonal elements are equal to  $1/(2m_0)$ .

### B. Basis functions

The  $n$ -electron explicitly correlated Gaussian functions are used to construct the spatial parts of the wave functions for the  $P$  and  $S$  states considered in this work. The  $S$ -type ECG functions have the following form:

$$\phi_k = \exp[-\mathbf{r}' (A_k \otimes \mathbf{I}) \mathbf{r}], \quad (4)$$

where

$$\mathbf{r} = \begin{pmatrix} \mathbf{r}_1 \\ \vdots \\ \mathbf{r}_n \end{pmatrix} \quad (5)$$

is a  $3n$ -component column vector consisting of  $n$  internal coordinate vectors,  $A_k$  is an  $n \times n$  positive-definite real symmetric matrix. The positive definiteness of  $A_k$  is required for ensuring that the wave function remains square integrable.

The  $P$ -type ECGs contain an additional prefactor before the Gaussian and read as follows:

$$\phi_k(\mathbf{r}) = z_{i_k} \exp[-\mathbf{r}' (A_k \otimes \mathbf{I}) \mathbf{r}]. \quad (6)$$

Here  $z_{i_k}$  is the  $z$  coordinate of the  $i$ th electron, while  $i_k$  is the electron label, which can vary in the  $(1, \dots, n)$  range.  $i_k$  represents an adjustable integer parameter in the calculations. This parameter is specific to each basis function and its value is determined variationally (i.e., based on how well the energy is improved) when the function is first added to the basis set. The  $z_{i_k}$  is a Cartesian spherical-harmonic angular prefactor that generates basis functions corresponding to the definite values of the total orbital angular momentum ( $L = 1$ ) and its projection on the  $z$  axis ( $M_L = 0$ ). A proper ( $L = 1, M_L = 0$ ) ECG is obtained regardless of the value of electron-label index  $i_k$ . Treating  $i_k$  as a variational parameter and optimizing it is optional. Due to indistinguishability of the electrons, choosing a fixed value of  $i_k$  (for example,  $i_k = 1$ ) and not optimizing it, but only optimizing the nonlinear exponential parameters (the elements of matrices  $A_k$ ), should, in principle, lead to the same outcome provided the optimization process is thorough and yields the global minimum. For more information on the ECG basis sets used in high-accuracy atomic calculations see [21,22,25,30].

### C. Oscillator strengths

In this work, we calculate the absorption oscillator strengths in both the length ( $L$ ) and velocity ( $V$ ) gauges. For a transition between initial state  $i$  and final state  $f$  they are expressed as follows [38,39]:

$$f_{if}^L = \frac{2}{3g_i} \Delta E_{if} |\boldsymbol{\mu}_{if}^L|^2, \quad |\boldsymbol{\mu}_{if}^L|^2 = |\langle \psi_i | \boldsymbol{\mu}^L | \psi_f \rangle|^2, \quad (7)$$

$$f_{if}^V = \frac{2}{3g_i \Delta E_{if}} |\boldsymbol{\mu}_{if}^V|^2, \quad |\boldsymbol{\mu}_{if}^V|^2 = |\langle \psi_i | \boldsymbol{\mu}^V | \psi_f \rangle|^2, \quad (8)$$

respectively, where  $g_i = 2J_i + 1$  is the statistical weight of the lower level ( $J_i$  is the total angular momentum quantum number),  $\Delta E_{if} = |E_i - E_f|$  is the nonrelativistic transition energy between the initial state  $\psi_i$  and final state  $\psi_f$ , and  $\boldsymbol{\mu}^L$  and  $\boldsymbol{\mu}^V$  are the transition dipole operators in the length and velocity gauge, respectively.

For an  $n$ -electron atom or, in general, for a Coulomb system with arbitrary charges and masses, the expressions for the transition dipole moments with respect to the origin located at the center of mass have the following form in the internal coordinates [40,41]:

$$\boldsymbol{\mu}^L = \sum_{i=1}^n \left( q_i - \frac{m_i}{m_{\text{tot}}} q_{\text{tot}} \right) \mathbf{r}_i \quad (9)$$

and

$$\boldsymbol{\mu}^V = \sum_{i=1}^n \left( \frac{q_0}{m_0} - \frac{q_i}{m_i} \right) \mathbf{p}_i, \quad (10)$$

where  $\mathbf{p}_i = -i \nabla_{r_i}$ ,  $q_{\text{tot}} = \sum_{i=0}^n q_i$  is the total charge of the system (zero for a neutral atom), and  $m_{\text{tot}} = \sum_{i=0}^n m_i$  is the total mass of the system. It should be noted that the above expressions for  $\boldsymbol{\mu}^L$  and  $\boldsymbol{\mu}^V$  are consistent with the Thomas-Reiche-Kuhn sum rule,

$$\sum_f f_{if} = n, \quad (11)$$

for any values of the charges and masses of the constituent particles and are certainly valid for all isotopes considered in this work.

As mentioned, due to the dependence of the internal Hamiltonian (2) on the nuclear mass, the resulting wave functions  $\psi_i$  and  $\psi_f$  also carry over the dependence on the nuclear mass. Thus, the wave functions for  ${}^{10}\text{B}$ ,  ${}^{11}\text{B}$ , and  ${}^{\infty}\text{B}$  are slightly different and the calculated oscillator strengths for the different isotopes are also slightly different. The degree of this dependence on the nuclear mass will be elucidated in Sec. III.

For the determination of oscillator strengths, only the matrix elements between the  $S$  ( $L = 0, M_L = 0$ ) and  $P$  ( $L = 1, M_L = 0$ ) states need to be evaluated (for more details see Sec. 2.4 in Ref. [23]). The expressions for the transition matrix elements in the length and velocity gauges with ECG basis functions (4) and (6) are available in our previous works [23,25].

It is noteworthy that some of the previous studies [42,43] have reported the line strength ( $S$ ). In the length gauge, the line strength ( $S^L$ ), oscillator strength ( $f^L$ ), and transition dipole

moment ( $\mu^L$ ) are related as follows:

$$f_{if}^L = \frac{2}{3g_i} \Delta E_{if} S^L, \quad S^L = |\mu_{if}^L|^2. \quad (12)$$

Tachiev and Froese Fischer have reported the line strengths in both the length ( $S^V$ ) and velocity ( $S^V$ ) gauges [44,45]. The latter one can be readily computed using the following relationship:

$$f_{if}^V = \frac{2}{3g_i} \Delta E_{if} S^V, \quad S^V = \frac{|\mu_{if}^V|^2}{\Delta E_{if}^2}. \quad (13)$$

To the best of the authors' knowledge, the transition dipole moments for B have never been reported by other research groups. They can serve as valuable data for benchmarking less accurate (and less computationally expensive) approaches. In this work, both the transition dipole moments and oscillator strengths will be presented in subsequent sections, as was done in our prior works [23,25]. Given the extensive data set in this study, the line strength values will not be included. Nevertheless, the latter quantity can be readily calculated from the transition dipole moment or the oscillator strength values using Eqs. (12) or (13).

### III. RESULTS

The lowest nine Rydberg  ${}^2P$  states and the lowest ten Rydberg  ${}^2S$  states of the boron atom are studied in this work. In the first step of the calculations, the nonrelativistic wave functions and the corresponding energies are obtained using the standard Rayleigh-Ritz variational method. In generating the ECG basis set for each state, the internal Hamiltonian corresponding to the  ${}^{11}\text{B}$  is used. The basis sets generated for all considered states of the  ${}^{11}\text{B}$  isotope are subsequently used to obtain the energies and the corresponding wave functions for  ${}^{10}\text{B}$  and  ${}^\infty\text{B}$ . Since the change of the wave function going from one isotope to another is rather small, it is not necessary to reoptimize basis sets for each isotope independently. A simple adjustment of the linear variational parameters by means of solving the generalized eigenvalue problem for a specific isotope is well sufficient for capturing this change.

The present calculations have been performed on three different computer clusters equipped with AMD EPYC 7642, AMD EPYC 7502, and Intel Xeon E5-2695v3 CPUs (central processing units) and used several hundreds of CPU cores at any given time. They lasted continuously for over a year with the largest fraction of CPU time spent on growing the basis set and optimizing the nonlinear parameters of the basis functions. The basis set was generated independently for each of the considered states of the boron atom, up to the size of 16 000 ECGs. The approach used in the optimization was described in our previous works (see, for example, Ref. [27]). Our code is written in FORTRAN and makes use of MPI (message passing interface) library to facilitate parallelism. Most of the calculations were performed using extended precision (also known as extended double precision or fp80), which represents float-point numbers with 80 bits of data (as opposed to 64 bits for the standard double precision, fp64). The use of the extended precision leads to slower calculations (typically by a factor of 5) but improves the quality of the optimization

and ensures notably better numerical stability, in particular, when very large basis sets are employed.

The linear and nonlinear parameters of all non-BO wave functions for the considered states of the boron atom generated in this work can be shared with the interested readers upon request.

#### A. Nonrelativistic energy

Table II shows the nonrelativistic energies ( $E_{\text{nr}}$ ) of the three  ${}^2P$  and three  ${}^2S$  states of  ${}^\infty\text{B}$  using basis sets with increasingly larger number of functions. Some of the most accurate values in the literature are also presented for comparison [33,34,46–50]. Generating nonrelativistic wave functions and corresponding energies is the most computationally demanding part of the calculations. It has taken a total of almost three years of continuous computing on a parallel computer system using many tens and even hundreds of cores at any given time. The calculations were performed with our in-house computer code, which makes use of the MPI (message passing interface) protocol for parallelism. By far the largest fraction of the computer time is spent to grow the basis set and optimize the nonlinear parameters of the Gaussians. The nonrelativistic variational calculations yield basis sets of progressively larger size in a process that involves growing the basis set from a small number of functions to its final size of 16 000 functions. The growing of the basis set for each state is performed independently from other states. The growing procedure involves adding new functions to the set and variationally optimizing their nonlinear parameters using a procedure that employs the analytical energy gradient determined with respect to these parameters. More details about the basis-set enlargement procedure can be found in our previous works [21,30].

It is clear from the table that, due to employing a very large number of ECGs in the wave-function expansion of each state, the calculated energies in this work are the most accurate nonrelativistic energies reported for boron atom to date. However, the high accuracy of the variational energies in this work is not solely due to employing larger number of ECG basis functions in calculations. A comparison of our nonrelativistic energies with the energies obtained in other ECG calculations (at the same basis size) shows that our energies are lower. We attribute this higher accuracy to the efficient optimization algorithm implemented in our code. For instance, the ground-state energy of  $-24.653\,867\,537$  hartree was obtained using 8192 ECGs by Puchalski *et al.* [33], while our calculation performed with 8000 ECGs yields a lower value of  $-24.653\,867\,60$  hartree. To the authors' knowledge, only the ground state of boron atom, i.e., the  ${}^2P$  state, has been investigated using ECBF by other groups [33,34] and there is no study with ECBF of any excited  ${}^2P$  or  ${}^2S$  states except for the ones previously reported by the present authors [26,27,31,51]. There have been some studies on the excited states with MCHF [44], MCSCF [47,52], and CI/Hy-CI [53] methods. However, the numerical uncertainties in the reported energies are orders of magnitude larger than the ones achieved in this work (see Table II).

In Table III, the nonrelativistic energies for all the  ${}^2S$  and  ${}^2P$  states considered in this study are provided. In this table two values have been shown for each state: the first



TABLE II. Convergence of the nonrelativistic energy (in atomic units) for several representative states of  ${}^\infty\text{B}$  obtained in this work. We also provide comparison with the best literature values obtained with various theoretical methods, i.e., the configuration interaction method (CI), the multiconfiguration interaction self-consistence field (MCSCF), the partitioned-correlation-function-interaction method (PCFI), the deconstrained partitioned-correlation-function-interaction method (DPCFI), the Hylleraas-CI method (Hy-CI), the diffusion Monte Carlo method (DMC), and the variational method employing the ECG basis functions. Some of the quoted energies are obtained by extrapolation to the infinite basis set limit.

State	Method	Ref.	Basis	$E_{\text{nr}}$	
$2\ ^2P$	Hy-CI	[46]	$N = 1158^{\text{a}}$	-24.648 145 22	
	MCSCF	[47]		-24.652 032	
	PCFI	[48]	$n = 10^{\text{b}}$	-24.653 464 335	
	DPCFI	[48]	$n = 10^{\text{b}}$	-24.653 523 595	
	DMC	[49]		-24.653 790 (3)	
	CI	[50]	$l_{\text{max}} = 20$	-24.653 837 33	
	CI	[50]	$\infty$	-23.653862(3)	
	ECG lobes	[34]	1873	-24.653 854 17	
		ECG	[33]	8192	-24.653 867 537
		ECG	[33]	$\infty$	-24.653 868 05(45)
		ECG	This work	6000	-24.653 866 85
		ECG	This work	8000	-24.653 867 60
		ECG	This work	10000	-24.653 868 03
		ECG	This work	12000	-24.653 868 27
		ECG	This work	14000	-24.653 868 42
ECG	This work	16000	-24.653 868 53		
ECG	This work	$\infty$	-24.653 868 66(13)		
$3\ ^2S$	MCSCF	[47]		-24.469 718	
	ECG	This work	6000	-24.471 393 30	
	ECG	This work	8000	-24.471 393 44	
	ECG	This work	10000	-24.471 393 52	
	ECG	This work	12000	-24.471 393 58	
	ECG	This work	14000	-24.471 393 61	
	ECG	This work	16000	-24.471 393 64	
ECG	This work	$\infty$	-24.471 393 68(4)		
$6\ ^2P$	ECG	This work	6000	-24.365 579 5	
	ECG	This work	8000	-24.365 584 1	
	ECG	This work	10000	-24.365 585 7	
	ECG	This work	12000	-24.365 586 4	
	ECG	This work	14000	-24.365 586 8	
	ECG	This work	16000	-24.365 587 6	
	ECG	This work	$\infty$	-24.365 588 4(8)	
$7\ ^2S$	ECG	This work	6000	-24.364 294 3	
	ECG	This work	8000	-24.364 315 6	
	ECG	This work	10000	-24.364 322 9	
	ECG	This work	12000	-24.364 326 4	
	ECG	This work	14000	-24.364 328 5	
	ECG	This work	16000	-24.364 331 2	
	ECG	This work	$\infty$	-24.364 334 5(33)	
$10\ ^2P$	ECG	This work	6000	-24.352 93	
	ECG	This work	8000	-24.353 04	
	ECG	This work	10000	-24.353 07	
	ECG	This work	12000	-24.354 34	
	ECG	This work	14000	-24.354 35	
	ECG	This work	16000	-24.354 40	
	ECG	This work	$\infty$	-24.354 450(53)	

TABLE II. (Continued.)

State	Method	Ref.	Basis	$E_{\text{nr}}$
$11\ ^2S$	ECG	This work	6000	-24.354 32
	ECG	This work	8000	-24.354 59
	ECG	This work	10000	-24.354 66
	ECG	This work	12000	-24.354 70
	ECG	This work	14000	-24.354 72
	ECG	This work	16000	-24.354 81
	ECG	This work	$\infty$	-24.354 92(11)

<sup>a</sup> $N$  is the total number of terms in the expansion.

<sup>b</sup> $n$  is the maximum principal quantum number of the orbitals used in the calculation.

one represents the variational energy computed using 16 000 ECG basis functions, while the second corresponds to the extrapolated energy derived from the energies obtained using 10 000–16 000 ECG basis functions (for more information about the extrapolation, see Ref. [27]). Furthermore, as one can see from the Tables II and III, the present variational calculations are well converged at the nonrelativistic level for all considered  ${}^2P$  and  ${}^2S$  states. However, due to the increased complexity of wave function with the increasing excitation level, there are fewer converged digits in the energy for higher states than for the lower ones. For example, for the lowest ( $2\ ^2P$ ) state and the highest ( $12\ ^2S$ ) state at least six and four digits after the decimal point are converged, respectively.

It should be noted that, in comparison with energy convergence rate for an atomic species with the same number of electrons, namely, the  $\text{C}^+$  ion [54], the convergence rate for boron atom is somewhat slower. The reason for this behavior can be found in a stronger configuration mixing in the boron atom than in the  $\text{C}^+$  ion. Also, the mixing is more significant for the  $S$  states (see Table I). For example, in the case of the  $2s\ 2p^2$  ( $7\ ^2S$ ) state, the contribution of the leading configuration decreases to 35%. While the ECG basis functions can handle this admixture of various configurations, it does slow down the convergence rate of the calculation. Lastly, a little higher nuclear charge value in the  $\text{C}^+$  ion makes the electron correlation effects somewhat less significant in relative terms.

It is worth noting that the lowest five  ${}^2S$  states of the boron atom were studied by our group before [27]. In that work we also used basis sets of up to 16 000 ECGs in the calculations. However, the computed energies and the corresponding uncertainties reported in this work are somewhat better converged. The improvement is achieved by performing several additional optimization cycles in the variational energy minimization of the ECGs. Consequently, the values of the nonrelativistic energies of the ground and excited states of the boron atom reported here should be considered more accurate compared to the energies reported in Ref. [27].

The main aim of this work is to calculate the oscillator strengths of all transitions between the considered  $S$  and  $P$  states of the two stable isotopes of the boron atom. The oscillator strengths are calculated at the nonrelativistic level of theory. Due to presence of the nuclear mass in the Hamiltonian (2), the nuclear mass effects are explicitly present in the calculated total energies and transition energies.

TABLE III. Nonrelativistic energies ( $E_{nr}$ ) obtained with the largest basis sets of 16 000 ECGs used in this work as well as the corresponding extrapolated values. The data for the lowest nine  ${}^2P$  and ten  ${}^2S$  states of the boron atom ( ${}^{10}\text{B}$ ,  ${}^{11}\text{B}$ , and  ${}^{\infty}\text{B}$ ) are presented. The values in parentheses are estimated uncertainties due to the extrapolation. All values are in atomic units.

State	Basis	${}^{10}\text{B}$	${}^{11}\text{B}$	${}^{\infty}\text{B}$	State	Basis	${}^{10}\text{B}$	${}^{11}\text{B}$	${}^{\infty}\text{B}$
$2^2P$	16000	-24.652 502 68	-24.652 626 32	-24.653 868 53	$3^2S$	16000	-24.470 019 349	-24.470 143 748	-24.471 393 641
	$\infty$	-24.652 502 81(13)	-24.652 626 45(13)	-24.653 868 66(13)		$\infty$	-24.470 019 386(38)	-24.470 143 786(38)	-24.471 393 679(38)
$3^2P$	16000	-24.430 973 92	-24.431 097 90	-24.432 343 61	$4^2S$	16000	-24.401 819 49	-24.401 943 49	-24.403 189 33
	$\infty$	-24.430 974 04(13)	-24.431 098 02(13)	-24.432 343 73(13)		$\infty$	-24.401 819 59(10)	-24.401 943 59(10)	-24.403 189 43(10)
$4^2P$	16000	-24.389 170 2	-24.389 294 0	-24.390 538 7	$5^2S$	16000	-24.378 424 0	-24.378 547 8	-24.379 791 9
	$\infty$	-24.389 170 30(17)	-24.389 294 20(17)	-24.390 538 90(17)		$\infty$	-24.378 424 30(31)	-24.378 548 20(31)	-24.379 792 20(31)
$5^2P$	16000	-24.372 547 54	-24.372 671 37	-24.373 915 48	$6^2S$	16000	-24.367 802 37	-24.367 925 89	-24.369 167 05
	$\infty$	-24.372 550 00(30)	-24.372 670 00(30)	-24.373 920 00(30)		$\infty$	-24.367 800 0(11)	-24.367 930 0(11)	-24.369 170 0(11)
$6^2P$	16000	-24.364 219 95	-24.364 343 75	-24.365 587 57	$7^2S$	16000	-24.362 977 53	-24.363 100 07	-24.364 331 19
	$\infty$	-24.364 220 75(80)	-24.364 344 55(80)	-24.365 588 37(80)		$\infty$	-24.362 980 9(33)	-24.363 103 4(33)	-24.364 334 5(33)
$7^2P$	16000	-24.359 451 53	-24.359 575 31	-24.360 818 96	$8^2S$	16000	-24.360 203 04	-24.360 326 18	-24.361 563 42
	$\infty$	-24.359 453 9(24)	-24.359 577 7(24)	-24.360 821 4(24)		$\infty$	-24.360 208 6(56)	-24.360 331 7(56)	-24.361 569 0(56)
$8^2P$	16000	-24.356 464 89	-24.356 588 66	-24.357 832 20	$9^2S$	16000	-24.357 249 41	-24.357 373 05	-24.358 615 29
	$\infty$	-24.356 475(10)	-24.356 599(10)	-24.357 842(10)		$\infty$	-24.357 265(16)	-24.357 389(16)	-24.358 631(16)
$9^2P$	16000	-24.354 458 31	-24.354 582 06	-24.355 825 53	$10^2S$	16000	-24.355 037 07	-24.355 160 79	-24.356 403 81
	$\infty$	-24.354 481(23)	-24.354 605(23)	-24.355 848(23)		$\infty$	-24.355 075(38)	-24.355 199(38)	-24.356 442(38)
$10^2P$	16000	-24.353 030 51	-24.353 154 26	-24.354 397 67	$11^2S$	16000	-24.353 441 13	-24.353 564 87	-24.354 808 08
	$\infty$	-24.353 083(53)	-24.353 207(53)	-24.354 450(53)		$\infty$	-24.353 55(11)	-24.353 67(11)	-24.354 92(11)
					$12^2S$	16000	-24.352 255 89	-24.352 379 63	-24.353 622 90
						$\infty$	-24.352 47(21)	-24.352 59(21)	-24.353 84(21)

Table IV shows the isotope-dependent transition energies obtained in this work, expressed in wave numbers (the hartree to  $\text{cm}^{-1}$  conversion factor adopted in this work is 219 474.631 363 20 [55]). The same extrapolation procedure as the one applied for the nonrelativistic energies has been used to obtain the nonrelativistic transition energies in the infinite basis-set limit. Rather than computing the total error as a root mean square of the individual uncertainties of the energies of the two states, we analyzed the convergence patterns of the energy difference and determined the total uncertainty based on that information. This is because the energies of both states involved in a transition are variational upper bounds and, thus, the corresponding errors partially cancel out when the difference is computed. The uncertainties due to the basis truncation error are small for the lower transitions (less than  $0.1 \text{ cm}^{-1}$ ) but increase with the excitation level.

Due to the absence of the relativistic and QED corrections, the accuracy of the nonrelativistic transition energies obtained in this work cannot be examined through a direct comparison with the available experimental data. Furthermore, comparatively low accuracy of the calculations reported in the literature makes them unsuitable for benchmarking the precision of the present data. In the work to follow we will present more accurate transition energies obtained with inclusion of the leading relativistic and QED corrections.

### B. Oscillator strengths

Table V shows how the oscillator strengths obtained in the length and velocity gauges converge with the size of the ECG basis set for some of the studied transitions. The data provide a good illustration of the convergence pattern that is observed for all transitions calculated in this work. As one can see, the obtained values are well converged for

lower transitions. For instance, the obtained values in the length and velocity gauges for  $2^2P \rightarrow 3^2S$  transition have six and seven significant figures converged, respectively. This is several orders of magnitude better than the previous reported results [42,44,56,57]. In all prior theoretical studies, only transitions between the low-lying  $S$  and  $P$  states were considered. Thus, for transitions involving higher-lying states, the oscillator strengths presented here are obtained in direct calculations. It should be mentioned that the previous most accurate calculations of the boron oscillator strengths have been performed using the mean-field approaches. Tachiev and Froese Fischer [44] employed the MCHF method to calculate the theoretical lifetimes for the  $2s^2 2p$ ,  $2s 2p^2$ ,  $2p^3$ ,  $2s^2 3s$ ,  $2s^2 3p$ ,  $2s^2 3d$ , and  $2s 2p 3s$  states. Later Fuhr and Wiese [42] computed the oscillator strengths for these states using the values reported by Tachiev and Froese Fischer and they estimated the uncertainties of their results. Another MCHF study by Wang *et al.* [56] on the spectra of the boron atom reported the oscillator strengths obtained in both the length and velocity gauges for the transitions between the  $2s^2 2p$ ,  $2s^2 3p$ , and  $2s^2 3s$ ,  $2s^2 3d$ ,  $2s^2 4s$ ,  $2s^2 4d$ ,  $2s^2 5s$  states. Recently, more accurate oscillator-strength values corresponding to the two gauges were calculated using the  $K$ -matrix method by Argenti and Moccia [57]. The values obtained in this work using the ECG basis functions are in agreement with the MCHF values [42,44] and the values obtained with the  $K$ -matrix method [57], while the uncertainty of our data is roughly 2–4 orders of magnitude smaller.

For instance, the values of  $7.869 26(13) \times 10^{-2}$  and  $7.869 368(68) \times 10^{-2}$  were obtained in this work for the  $2^2P \rightarrow 3^2S$  transition using the length and velocity gauges, respectively. They are in good agreement with the value of  $7.83(23) \times 10^{-2}$  calculated in the length gauge using the MCHF method [42,44] and values of  $7.87 \times 10^{-2}$  and

TABLE IV. Nonrelativistic transition energies ( $\Delta E_{nr}$ ) for the lowest nine  ${}^2P$  and ten  ${}^2S$  states of the boron atom ( ${}^{10}\text{B}$ ,  ${}^{11}\text{B}$ , and  ${}^{\infty}\text{B}$ ). All values are in  $\text{cm}^{-1}$ . The uncertainty estimates due to the extrapolation are shown in parentheses.

Transition	${}^{10}\text{B}$	${}^{11}\text{B}$	${}^{\infty}\text{B}$	Transition	${}^{10}\text{B}$	${}^{11}\text{B}$	${}^{\infty}\text{B}$
$2\ {}^2P \rightarrow 3\ {}^2S$	40050.484(22)	40050.316(22)	40048.630(22)	$2\ {}^2P \rightarrow 4\ {}^2S$	55018.609(8)	55018.530(8)	55017.732(8)
$2\ {}^2P \rightarrow 5\ {}^2S$	60153.266(46)	60153.226(46)	60152.821(46)	$2\ {}^2P \rightarrow 6\ {}^2S$	62484.23(26)	62484.26(26)	62484.49(26)
$2\ {}^2P \rightarrow 7\ {}^2S$	63542.57(86)	63542.81(86)	63545.24(86)	$2\ {}^2P \rightarrow 8\ {}^2S$	64151.2(11)	64151.3(11)	64152.4(11)
$2\ {}^2P \rightarrow 9\ {}^2S$	64797.2(34)	64797.2(34)	64797.2(34)	$2\ {}^2P \rightarrow 10\ {}^2S$	65278.8(74)	65278.7(74)	65278.6(74)
$2\ {}^2P \rightarrow 11\ {}^2S$	65616(21)	65616(21)	65615(21)	$2\ {}^2P \rightarrow 12\ {}^2S$	65850(47)	65850(47)	65849(47)
$3\ {}^2P \rightarrow 3\ {}^2S$	8569.462(20)	8569.553(20)	8570.472(20)	$3\ {}^2P \rightarrow 4\ {}^2S$	6398.665(7)	6398.662(7)	6398.632(7)
$3\ {}^2P \rightarrow 5\ {}^2S$	11533.316(52)	11533.352(52)	11533.715(52)	$3\ {}^2P \rightarrow 6\ {}^2S$	13864.28(28)	13864.38(28)	13865.37(28)
$3\ {}^2P \rightarrow 7\ {}^2S$	14922.62(87)	14922.93(87)	14926.14(87)	$3\ {}^2P \rightarrow 8\ {}^2S$	15530.9(15)	15531.1(15)	15533.0(15)
$3\ {}^2P \rightarrow 9\ {}^2S$	16176.9(37)	16177.0(37)	16177.8(37)	$3\ {}^2P \rightarrow 10\ {}^2S$	16658.1(81)	16658.2(81)	16658.8(81)
$3\ {}^2P \rightarrow 11\ {}^2S$	16996(21)	16996(21)	16996(21)	$3\ {}^2P \rightarrow 12\ {}^2S$	17226(51)	17226(51)	17226(51)
$4\ {}^2P \rightarrow 3\ {}^2S$	17744.300(43)	17744.415(43)	17745.569(43)	$4\ {}^2P \rightarrow 4\ {}^2S$	2776.183(21)	2776.210(21)	2776.475(21)
$4\ {}^2P \rightarrow 5\ {}^2S$	2358.468(38)	2358.481(38)	2358.608(38)	$4\ {}^2P \rightarrow 6\ {}^2S$	4689.43(27)	4689.50(27)	4690.26(27)
$4\ {}^2P \rightarrow 7\ {}^2S$	5747.75(87)	5748.05(87)	5751.01(87)	$4\ {}^2P \rightarrow 8\ {}^2S$	6356.1(15)	6356.2(15)	6357.8(15)
$4\ {}^2P \rightarrow 9\ {}^2S$	7002.4(34)	7002.4(34)	7003.0(34)	$4\ {}^2P \rightarrow 10\ {}^2S$	7482.6(87)	7482.7(87)	7483.0(87)
$4\ {}^2P \rightarrow 11\ {}^2S$	7821(21)	7821(21)	7821(21)	$4\ {}^2P \rightarrow 12\ {}^2S$	8051(51)	8051(51)	8051(51)
$5\ {}^2P \rightarrow 3\ {}^2S$	21392.515(74)	21392.641(74)	21393.912(74)	$5\ {}^2P \rightarrow 4\ {}^2S$	6424.30(15)	6424.34(15)	6424.72(15)
$5\ {}^2P \rightarrow 5\ {}^2S$	1289.751(12)	1289.750(12)	1289.736(12)	$5\ {}^2P \rightarrow 6\ {}^2S$	1041.26(18)	1041.33(18)	1041.98(18)
$5\ {}^2P \rightarrow 7\ {}^2S$	2099.56(81)	2099.85(81)	2102.70(81)	$5\ {}^2P \rightarrow 8\ {}^2S$	2707.8(15)	2707.9(15)	2709.4(15)
$5\ {}^2P \rightarrow 9\ {}^2S$	3354.2(34)	3354.2(34)	3354.6(34)	$5\ {}^2P \rightarrow 10\ {}^2S$	3835.1(80)	3835.1(80)	3835.3(80)
$5\ {}^2P \rightarrow 11\ {}^2S$	4173(21)	4173(21)	4173(21)	$5\ {}^2P \rightarrow 12\ {}^2S$	4407(47)	4407(47)	4407(47)
$6\ {}^2P \rightarrow 3\ {}^2S$	23220.09(20)	23220.22(20)	23221.55(20)	$6\ {}^2P \rightarrow 4\ {}^2S$	8251.96(19)	8252.00(19)	8252.44(19)
$6\ {}^2P \rightarrow 5\ {}^2S$	3117.29(15)	3117.29(15)	3117.34(15)	$6\ {}^2P \rightarrow 6\ {}^2S$	786.281(32)	786.222(32)	785.637(32)
$6\ {}^2P \rightarrow 7\ {}^2S$	271.94(74)	272.22(74)	275.01(74)	$6\ {}^2P \rightarrow 8\ {}^2S$	880.4(12)	880.5(12)	882.0(12)
$6\ {}^2P \rightarrow 9\ {}^2S$	1526.7(32)	1526.7(32)	1527.1(32)	$6\ {}^2P \rightarrow 10\ {}^2S$	2008.3(71)	2008.3(71)	2008.5(71)
$6\ {}^2P \rightarrow 11\ {}^2S$	2343(22)	2343(22)	2344(22)	$6\ {}^2P \rightarrow 12\ {}^2S$	2585(41)	2585(41)	2585(41)
$7\ {}^2P \rightarrow 3\ {}^2S$	24266.21(62)	24266.35(62)	24267.72(62)	$7\ {}^2P \rightarrow 4\ {}^2S$	9298.11(58)	9298.16(58)	9298.64(58)
$7\ {}^2P \rightarrow 5\ {}^2S$	4163.42(56)	4163.43(56)	4163.52(56)	$7\ {}^2P \rightarrow 6\ {}^2S$	1832.45(35)	1832.39(35)	1831.84(35)
$7\ {}^2P \rightarrow 7\ {}^2S$	773.919(52)	773.646(52)	770.899(52)	$7\ {}^2P \rightarrow 8\ {}^2S$	165.78(84)	165.64(84)	164.23(84)
$7\ {}^2P \rightarrow 9\ {}^2S$	480.6(27)	480.6(27)	480.9(27)	$7\ {}^2P \rightarrow 10\ {}^2S$	962.3(65)	962.3(65)	962.5(65)
$7\ {}^2P \rightarrow 11\ {}^2S$	1299(20)	1299(20)	1299(20)	$7\ {}^2P \rightarrow 12\ {}^2S$	1533(46)	1533(46)	1534(46)
$8\ {}^2P \rightarrow 3\ {}^2S$	24919.5(29)	24919.6(29)	24921.0(29)	$8\ {}^2P \rightarrow 4\ {}^2S$	9951.7(25)	9951.7(25)	9952.2(25)
$8\ {}^2P \rightarrow 5\ {}^2S$	4816.8(27)	4816.8(27)	4816.9(27)	$8\ {}^2P \rightarrow 6\ {}^2S$	2486.0(23)	2486.0(23)	2485.4(23)
$8\ {}^2P \rightarrow 7\ {}^2S$	1427.5(19)	1427.2(19)	1424.5(19)	$8\ {}^2P \rightarrow 8\ {}^2S$	819.1(13)	819.0(13)	817.6(13)
$8\ {}^2P \rightarrow 9\ {}^2S$	173.00(82)	172.97(82)	172.69(82)	$8\ {}^2P \rightarrow 10\ {}^2S$	307.3(61)	307.3(61)	307.4(61)
$8\ {}^2P \rightarrow 11\ {}^2S$	641(23)	641(23)	641(23)	$8\ {}^2P \rightarrow 12\ {}^2S$	880(44)	880(44)	880(44)
$9\ {}^2P \rightarrow 3\ {}^2S$	25357.1(56)	25357.2(56)	25358.6(56)	$9\ {}^2P \rightarrow 4\ {}^2S$	10389.0(56)	10389.0(56)	10389.6(56)
$9\ {}^2P \rightarrow 5\ {}^2S$	5254.4(55)	5254.4(55)	5254.5(55)	$9\ {}^2P \rightarrow 6\ {}^2S$	2922.9(57)	2922.9(57)	2922.4(57)
$9\ {}^2P \rightarrow 7\ {}^2S$	1864.8(50)	1864.5(50)	1861.8(50)	$9\ {}^2P \rightarrow 8\ {}^2S$	1256.4(44)	1256.3(44)	1254.9(44)
$9\ {}^2P \rightarrow 9\ {}^2S$	611.81(77)	611.78(77)	611.51(77)	$9\ {}^2P \rightarrow 10\ {}^2S$	129.0(16)	129.0(16)	129.0(16)
$9\ {}^2P \rightarrow 11\ {}^2S$	204(19)	204(19)	204(19)	$9\ {}^2P \rightarrow 12\ {}^2S$	444(39)	444(39)	444(39)
$10\ {}^2P \rightarrow 3\ {}^2S$	25662(14)	25662(14)	25663(14)	$10\ {}^2P \rightarrow 4\ {}^2S$	10694(14)	10694(14)	10694(14)
$10\ {}^2P \rightarrow 5\ {}^2S$	5562(11)	5562(11)	5562(11)	$10\ {}^2P \rightarrow 6\ {}^2S$	3229(13)	3229(13)	3228(13)
$10\ {}^2P \rightarrow 7\ {}^2S$	2170(13)	2170(13)	2167(13)	$10\ {}^2P \rightarrow 8\ {}^2S$	1562(12)	1562(12)	1560(12)
$10\ {}^2P \rightarrow 9\ {}^2S$	914(12)	914(12)	914(12)	$10\ {}^2P \rightarrow 10\ {}^2S$	434.0(65)	434.0(65)	434.0(65)
$10\ {}^2P \rightarrow 11\ {}^2S$	98.9(88)	98.9(88)	98.9(88)	$10\ {}^2P \rightarrow 12\ {}^2S$	132(38)	132(38)	133(38)

$7.61 \times 10^{-2}$  obtained by the  $K$ -matrix method in the length and velocity gauges [57]. In the case of the aforementioned transition, our values calculated using different gauges agree to within 4 digits and both values are within the estimated uncertainty range of each other, while such an agreement is not seen in the MCHF values [44,56] or the values obtained with the  $K$ -matrix method [57] (see Table V).

In general, it appears that the values obtained with the  $K$ -matrix method [57] are more accurate than the MCHF values [44]. For example, in the case of  $4\ {}^2P \rightarrow 9\ {}^2S$  transi-

tion, the  $5.36 \times 10^{-3}$  and  $5.17 \times 10^{-3}$  values obtained in the length and velocity gauges, respectively, are in good agreement with the values obtained in this work [ $5.154(20) \times 10^{-3}$  and  $5.156(25) \times 10^{-3}$ ] while the MCHF value obtained in Refs. [42,44] ( $3.03 \times 10^{-3}$ ) is very far from the values obtained using the two former methods.

Efforts to enhance the accuracy of the results may include alternative approaches to estimating the uncertainties. Utilizing the theoretical framework of Weinhold and others [58–60], rigorous upper and lower bounds for the oscillator

TABLE V. Nonrelativistic absorption oscillator strengths in length ( $f^L$ ) and velocity gauges ( $f^V$ ) for some of the studied transitions obtained for the case of an infinite nuclear mass ( $^\infty\text{B}$ ). The oscillator strength uncertainties (given in parentheses) are computed as root mean squares of the uncertainties of  $|\mu_{if}^L|^2$  or  $|\mu_{if}^V|^2$  and  $\Delta E_{if}$ , where  $\Delta E_{if}$  is the difference between the nonrelativistic energies of the initial ( $i$ ) and final ( $f$ ) states. The calculations in Ref. [44] were performed in the framework of the nonrelativistic multiconfiguration Hartree-Fock (MCHF) method. The uncertainty is calculated based on procedure in Ref. [42].

Basis( $S$ )	Basis( $P$ )	$f^L$	$f^V$
$2^2P \rightarrow 3^2S$			
10000	10000	$7.868\,713 \times 10^{-2}$	$7.869\,260 \times 10^{-2}$
12000	12000	$7.868\,999 \times 10^{-2}$	$7.869\,218 \times 10^{-2}$
14000	14000	$7.869\,045 \times 10^{-2}$	$7.869\,302 \times 10^{-2}$
16000	16000	$7.869\,130 \times 10^{-2}$	$7.869\,312 \times 10^{-2}$
$\infty$	$\infty$	$7.869\,25(13) \times 10^{-2}$	$7.869\,350(42) \times 10^{-2}$
MCHF [42,44]		$7.83(23) \times 10^{-2}$	
MCHF [51]		$7.83(23) \times 10^{-2}$	
$K$ matrix [52]		$7.87 \times 10^{-2}$	$7.61 \times 10^{-2}$
$3^2S \rightarrow 3^2P$			
10000	10000	1.051 866 16	1.051 793 57
12000	12000	1.051 861 94	1.051 793 69
14000	14000	1.051 859 29	1.051 799 38
16000	16000	1.051 856 80	1.051 809 77
$\infty$	$\infty$	1.0518 53 7(26)	1.051 827(15)
MCHF [42,44]		1.05(11)	
MCHF [51]		1.07	1.08
$K$ matrix [52]		1.05	1.04
$4^2P \rightarrow 9^2S$			
10000	13000	$5.191\,31 \times 10^{-3}$	$5.195\,57 \times 10^{-3}$
12000	14000	$5.192\,33 \times 10^{-3}$	$5.194\,02 \times 10^{-3}$
14000	15000	$5.189\,78 \times 10^{-3}$	$5.192\,19 \times 10^{-3}$
16000	16000	$5.176\,49 \times 10^{-3}$	$5.181\,17 \times 10^{-3}$
$\infty$	$\infty$	$5.157(17) \times 10^{-3}$	$5.164(20) \times 10^{-3}$
MCHF [42,44]		$3.03(76) \times 10^{-3}$	
$K$ matrix [52]		$5.36 \times 10^{-3}$	$5.2 \times 10^{-3}$
$9^2S \rightarrow 8^2P$			
10000	13000	2.722 931 08	2.707 138 75
12000	14000	2.713 436 27	2.713 636 18
14000	15000	2.708 979 74	2.716 802 64
16000	16000	2.707 481 31	2.717 366 01
$\infty$	$\infty$	2.707(19)	2.719(19)
$9^2P \rightarrow 11^2S$			
10000	13000	$8.493\,073\,7 \times 10^{-1}$	$7.237\,994\,1 \times 10^{-1}$
12000	14000	$8.393\,109\,7 \times 10^{-1}$	$7.278\,517\,5 \times 10^{-1}$
14000	15000	$8.327\,723\,4 \times 10^{-1}$	$7.312\,693\,2 \times 10^{-1}$
16000	16000	$8.302\,581\,0 \times 10^{-1}$	$7.746\,667\,6 \times 10^{-1}$
$\infty$	$\infty$	$8.10(90) \times 10^{-1}$	$8.52(79) \times 10^{-1}$

strength ( $f$ ) can be computed in accordance with nonrelativistic quantum mechanical tenets. These bounds have been previously delineated for both atomic and molecular oscillator strengths in Refs. [61,62]. Despite their theoretical rigor, further analyses have revealed that the bounds calculated using this approach may not accurately reflect the true precision of the calculated oscillator strengths (for more information see Refs. [62,63]). For instance,  $7.834\,988 \times 10^{-2}$  and  $7.903\,273 \times 10^{-2}$  values are estimated as a lower bound and upper bound for the  $2^2P \rightarrow 3^2S$  transition of  $^\infty\text{B}$ , respectively. In comparison with the calculated values using the ECG method ( $7.869\,252 \times 10^{-2}$ ), these have a significantly broader error bar ( $\pm 3.4 \times 10^{-4}$ ) than those obtained from the extrapolation ( $\pm 1.3 \times 10^{-6}$ ). We conclude that the uncertainty values derived from the upper-lower bounds approach do not tighten the estimated uncertainty ranges. Thus, in our calculations, they do not have any practical value.

In Tables VI and VII, we show the calculated values of the transition matrix elements and the oscillator strengths of the  $S \rightarrow P$  and  $P \rightarrow S$  transitions for the  $^{10}\text{B}$  and  $^{11}\text{B}$  isotopes, and for the boron atom with an infinite nuclear mass ( $^\infty\text{B}$ ). The oscillator strengths are calculated for all states considered in this work. In the two tables, only the extrapolated values obtained from the calculated oscillator strengths using 10 000–16 000 ECGs are shown. The uncertainties shown in Table VI are due to the basis-set truncation error. The uncertainties shown in Table VII are calculated as the root mean squares of the uncertainties of  $|\mu_{if}|^2$  and  $\Delta E$ . The oscillator strengths are compared with the available literature results.

In general, the agreement between the oscillator strengths calculated in this work and the available literature values correlates well with the accuracy of the method used to generate the wave functions. This work not only provides benchmark values for the oscillator strengths, but reports them for a considerably wider range of the  $S$ - $P$  transitions compared to the previous computational studies. Moreover, we compute the transition dipole moments and the corresponding oscillator strengths for the two isotopes of boron. The obtained oscillator strengths revealed that, while for some of the excited states more accurate wave functions are needed to more clearly distinguish the isotopes, for the rest of the states the results seem reliable enough to make the distinction. It should be noted that while up to this point experimental measurements have not been precise enough to discriminate between the oscillator strengths of the two boron isotopes, this may become feasible in the future.

The oscillator strengths for all transitions considered in this work are shown graphically in logarithmic scale in Figs. 1(a) and 1(b) for  $^{11}\text{B}$  in the length and velocity gauges, respectively. Both the tabulated oscillator strengths and their depiction show that for  $^{10}\text{B}$  and  $^{11}\text{B}$  isotopes, as well as  $^\infty\text{B}$ , the largest values of the strengths correspond to transitions between  $S$  and  $P$  states with the same principal quantum number, i.e., the  $2s^2 np \rightarrow 2s^2 ns$  and  $2s^2 ns \rightarrow 2s^2 np$  transitions. It is worth mentioning that the calculated oscillator strengths for the  $n^2P \rightarrow (n+1)^2S$  transitions have comparable values as those for the transitions between two states with same principal quantum number. This indicates a possibility to use a  $P \rightarrow S \rightarrow P \rightarrow S \dots$  “cascade” excitation sequence to prepare a boron atom in a particular Rydberg state.



TABLE VI. The squares of the absorption transition dipole matrix elements, in the length ( $|\mu_{ij}^L|^2$ ) and velocity forms ( $|\mu_{ij}^V|^2$ ) for the transitions involving  ${}^2S$  and  ${}^2P$  states. The numbers in parentheses are estimated uncertainties due to the basis truncation. In those instances where the uncertainty exceeds the reported value [e.g.,  $a(b) \equiv a_{-b}^{+b}$  with  $b > a$ ], which would make the lower bound to be a negative number, the lower bound should be assumed to be zero (i.e.,  $a_{-a}^{+b}$ ). All values are in atomic units.

Transition	$ \mu_{ij}^L ^2({}^{10}\text{B})$	$ \mu_{ij}^L ^2({}^{11}\text{B})$	$ \mu_{ij}^L ^2({}^{\infty}\text{B})$	$ \mu_{ij}^V ^2({}^{10}\text{B})$	$ \mu_{ij}^V ^2({}^{11}\text{B})$	$ \mu_{ij}^V ^2({}^{\infty}\text{B})$
${}^2P \rightarrow {}^3S$	3.881 115(58)	3.881 129(58)	3.881 259(58)	$1.292\,427\,9(70) \times 10^{-1}$	$1.292\,420\,9(70) \times 10^{-1}$	$1.292\,363\,5(70) \times 10^{-1}$
${}^2P \rightarrow {}^4S$	$5.907\,99(73) \times 10^{-1}$	$5.907\,80(73) \times 10^{-1}$	$5.905\,88(73) \times 10^{-1}$	$3.712\,293(40) \times 10^{-2}$	$3.712\,162(40) \times 10^{-2}$	$3.710\,840(40) \times 10^{-2}$
${}^2P \rightarrow {}^5S$	$3.624\,83(39) \times 10^{-1}$	$3.624\,33(39) \times 10^{-1}$	$3.619\,39(39) \times 10^{-1}$	$2.722\,98(42) \times 10^{-2}$	$2.722\,60(42) \times 10^{-2}$	$2.718\,84(42) \times 10^{-2}$
${}^2P \rightarrow {}^6S$	$5.316\,8(12) \times 10^{-1}$	$5.314\,4(12) \times 10^{-1}$	$5.291\,9(12) \times 10^{-1}$	$4.309\,43(93) \times 10^{-2}$	$4.307\,59(93) \times 10^{-2}$	$4.289\,18(93) \times 10^{-2}$
${}^2P \rightarrow {}^7S$	1.187 87(62)	1.187 98(62)	1.188 90(62)	$9.957\,5(95) \times 10^{-2}$	$9.958\,2(95) \times 10^{-2}$	$9.962\,4(95) \times 10^{-2}$
${}^2P \rightarrow {}^8S$	$3.882\,6(21) \times 10^{-1}$	$3.888\,9(21) \times 10^{-1}$	$3.951\,9(21) \times 10^{-1}$	$3.317\,9(12) \times 10^{-2}$	$3.323\,2(12) \times 10^{-2}$	$3.377\,0(12) \times 10^{-2}$
${}^2P \rightarrow {}^9S$	$4.736\,9(49) \times 10^{-2}$	$4.745\,1(49) \times 10^{-2}$	$4.828\,5(49) \times 10^{-2}$	$4.128\,5(42) \times 10^{-3}$	$4.135\,6(42) \times 10^{-3}$	$4.207\,8(42) \times 10^{-3}$
${}^2P \rightarrow {}^{10}S$	$1.029\,9(80) \times 10^{-2}$	$1.031\,8(80) \times 10^{-2}$	$1.051\,3(80) \times 10^{-2}$	$9.106(70) \times 10^{-4}$	$9.123(70) \times 10^{-4}$	$9.294(70) \times 10^{-4}$
${}^2P \rightarrow {}^{11}S$	$3.29(10) \times 10^{-3}$	$3.29(10) \times 10^{-3}$	$3.37(10) \times 10^{-3}$	$2.932(95) \times 10^{-4}$	$2.938(95) \times 10^{-4}$	$3.002(95) \times 10^{-4}$
${}^2P \rightarrow {}^{12}S$	$1.358(56) \times 10^{-3}$	$1.361(56) \times 10^{-3}$	$1.395(56) \times 10^{-3}$	$1.217(47) \times 10^{-4}$	$1.219(47) \times 10^{-4}$	$1.249(47) \times 10^{-4}$
${}^3S \rightarrow {}^3P$	$8.081\,817\,0(54) \times 10^1$	$8.081\,728\,1(54) \times 10^1$	$8.080\,833\,6(54) \times 10^1$	$1.232\,132(15) \times 10^{-1}$	$1.232\,139(14) \times 10^{-1}$	$1.232\,213(17) \times 10^{-1}$
${}^3S \rightarrow {}^4P$	$9.573\,9(37) \times 10^{-2}$	$9.575\,3(37) \times 10^{-2}$	$9.589\,6(37) \times 10^{-2}$	$6.255\,9(10) \times 10^{-4}$	$6.256\,9(10) \times 10^{-4}$	$6.267\,3(10) \times 10^{-4}$
${}^3S \rightarrow {}^5P$	$3.70(15) \times 10^{-5}$	$3.68(15) \times 10^{-5}$	$3.48(15) \times 10^{-5}$	$3.362(30) \times 10^{-7}$	$3.344(30) \times 10^{-7}$	$3.165(30) \times 10^{-7}$
${}^3S \rightarrow {}^6P$	$2.597\,3(78) \times 10^{-3}$	$2.596\,0(78) \times 10^{-3}$	$2.583\,8(78) \times 10^{-3}$	$2.897\,3(22) \times 10^{-5}$	$2.896\,1(22) \times 10^{-5}$	$2.883\,7(20) \times 10^{-5}$
${}^3S \rightarrow {}^7P$	$3.088\,9(76) \times 10^{-3}$	$3.087\,8(76) \times 10^{-3}$	$3.077\,1(76) \times 10^{-3}$	$3.775(10) \times 10^{-5}$	$3.774(10) \times 10^{-5}$	$3.762(10) \times 10^{-5}$
${}^3S \rightarrow {}^8P$	$2.682(17) \times 10^{-3}$	$2.682(17) \times 10^{-3}$	$2.673(17) \times 10^{-3}$	$3.462(20) \times 10^{-5}$	$3.461(20) \times 10^{-5}$	$3.452(20) \times 10^{-5}$
${}^3S \rightarrow {}^9P$	$2.136(11) \times 10^{-3}$	$2.135(11) \times 10^{-3}$	$2.128(11) \times 10^{-3}$	$2.856(10) \times 10^{-5}$	$2.855(10) \times 10^{-5}$	$2.847(10) \times 10^{-5}$
${}^3S \rightarrow {}^{10}P$	$1.679(10) \times 10^{-3}$	$1.678(10) \times 10^{-3}$	$1.674(10) \times 10^{-3}$	$2.299\,0(40) \times 10^{-5}$	$2.298\,5(40) \times 10^{-5}$	$2.293\,0(40) \times 10^{-5}$
${}^3P \rightarrow {}^4S$	$6.219\,354(11) \times 10^1$	$6.219\,390(11) \times 10^1$	$6.219\,510(11) \times 10^1$	$5.286\,234(60) \times 10^{-2}$	$5.286\,252(60) \times 10^{-2}$	$5.286\,418(60) \times 10^{-2}$
${}^3P \rightarrow {}^5S$	3.501 90(78)	3.501 89(78)	3.501 87(78)	$9.666\,72(50) \times 10^{-3}$	$9.666\,77(50) \times 10^{-3}$	$9.667\,22(50) \times 10^{-3}$
${}^3P \rightarrow {}^6S$	$8.411\,5(88) \times 10^{-1}$	$8.412\,7(88) \times 10^{-1}$	$8.425\,6(88) \times 10^{-1}$	$3.361\,4(11) \times 10^{-3}$	$3.361\,9(11) \times 10^{-3}$	$3.367\,4(13) \times 10^{-3}$
${}^3P \rightarrow {}^7S$	$3.474(17) \times 10^{-2}$	$3.490(17) \times 10^{-2}$	$3.652(17) \times 10^{-2}$	$1.604\,8(60) \times 10^{-4}$	$1.612\,2(50) \times 10^{-4}$	$1.689\,6(60) \times 10^{-4}$
${}^3P \rightarrow {}^8S$	$1.844\,9(50) \times 10^{-1}$	$1.843\,2(50) \times 10^{-1}$	$1.826\,6(50) \times 10^{-1}$	$9.250(18) \times 10^{-4}$	$9.242(19) \times 10^{-4}$	$9.162(20) \times 10^{-4}$
${}^3P \rightarrow {}^9S$	$1.917\,3(71) \times 10^{-1}$	$1.917\,2(71) \times 10^{-1}$	$1.915\,8(71) \times 10^{-1}$	$1.042\,3(38) \times 10^{-3}$	$1.042\,3(39) \times 10^{-3}$	$1.041\,8(40) \times 10^{-3}$
${}^3P \rightarrow {}^{10}S$	$1.293(13) \times 10^{-1}$	$1.293(13) \times 10^{-1}$	$1.292(13) \times 10^{-1}$	$7.445(79) \times 10^{-4}$	$7.445(79) \times 10^{-4}$	$7.444(79) \times 10^{-4}$
${}^3P \rightarrow {}^{11}S$	$8.72(38) \times 10^{-2}$	$8.72(38) \times 10^{-2}$	$8.72(38) \times 10^{-2}$	$5.21(25) \times 10^{-4}$	$5.21(25) \times 10^{-4}$	$5.21(25) \times 10^{-4}$
${}^3P \rightarrow {}^{12}S$	$6.27(38) \times 10^{-2}$	$6.27(38) \times 10^{-2}$	$6.26(38) \times 10^{-2}$	$3.83(28) \times 10^{-4}$	$3.83(28) \times 10^{-4}$	$3.83(28) \times 10^{-4}$
${}^4S \rightarrow {}^4P$	$3.643\,985\,4(59) \times 10^2$	$3.643\,947\,2(60) \times 10^2$	$3.643\,563\,6(61) \times 10^2$	$5.830\,72(14) \times 10^{-2}$	$5.830\,72(14) \times 10^{-2}$	$5.830\,68(17) \times 10^{-2}$
${}^4S \rightarrow {}^5P$	1.681 16(66)	1.68124(67)	1.682 03(74)	$1.439\,47(30) \times 10^{-3}$	$1.439\,52(30) \times 10^{-3}$	$1.440\,10(30) \times 10^{-3}$
${}^4S \rightarrow {}^6P$	$1.395\,0(41) \times 10^1$	$1.395\,2(41) \times 10^1$	$1.396\,8(41) \times 10^1$	$1.979\,2(10) \times 10^{-4}$	$1.979\,3(10) \times 10^{-4}$	$1.981\,1(10) \times 10^{-4}$
${}^4S \rightarrow {}^7P$	$2.561\,0(74) \times 10^{-2}$	$2.562\,0(68) \times 10^{-2}$	$2.566\,1(72) \times 10^{-2}$	$4.595(10) \times 10^{-5}$	$4.595(10) \times 10^{-5}$	$4.602(10) \times 10^{-5}$
${}^4S \rightarrow {}^8P$	$6.880(52) \times 10^{-3}$	$6.881(52) \times 10^{-3}$	$6.899(52) \times 10^{-3}$	$1.399(10) \times 10^{-5}$	$1.398(10) \times 10^{-5}$	$1.402(10) \times 10^{-5}$
${}^4S \rightarrow {}^9P$	$2.420(25) \times 10^{-3}$	$2.421(24) \times 10^{-3}$	$2.430(23) \times 10^{-3}$	$5.35(10) \times 10^{-6}$	$5.34(10) \times 10^{-6}$	$5.36(10) \times 10^{-6}$
${}^4S \rightarrow {}^{10}P$	$9.97(35) \times 10^{-4}$	$9.96(36) \times 10^{-4}$	$1.00(37) \times 10^{-3}$	$2.22(20) \times 10^{-6}$	$2.22(20) \times 10^{-6}$	$2.23(20) \times 10^{-6}$
${}^4P \rightarrow {}^5S$	$2.785\,007(41) \times 10^2$	$2.784\,997(41) \times 10^2$	$2.784\,892(42) \times 10^2$	$3.215\,865(50) \times 10^{-2}$	$3.215\,876(50) \times 10^{-2}$	$3.216\,089(50) \times 10^{-2}$
${}^4P \rightarrow {}^6S$	9.730 1(83)	9.732 1(84)	9.751 4(87)	$4.438\,7(16) \times 10^{-3}$	$4.439\,6(16) \times 10^{-3}$	$4.449\,8(16) \times 10^{-3}$
${}^4P \rightarrow {}^7S$	$3.13(17) \times 10^{-3}$	$3.28(17) \times 10^{-3}$	$4.97(19) \times 10^{-3}$	$2.19(10) \times 10^{-6}$	$2.29(10) \times 10^{-6}$	$3.44(10) \times 10^{-6}$
${}^4P \rightarrow {}^8S$	2.183 88(86)	2.182 71(84)	2.170 5(10)	$1.829\,4(33) \times 10^{-3}$	$1.828\,5(34) \times 10^{-3}$	$1.819\,4(43) \times 10^{-3}$
${}^4P \rightarrow {}^9S$	1.454 1(47)	1.454 2(47)	1.454 5(49)	$1.482\,1(56) \times 10^{-3}$	$1.482\,2(56) \times 10^{-3}$	$1.482\,9(57) \times 10^{-3}$
${}^4P \rightarrow {}^{10}S$	$8.151(88) \times 10^{-1}$	$8.151(88) \times 10^{-1}$	$8.154(88) \times 10^{-1}$	$9.48(10) \times 10^{-4}$	$9.48(10) \times 10^{-4}$	$9.48(10) \times 10^{-4}$
${}^4P \rightarrow {}^{11}S$	$4.94(24) \times 10^{-1}$	$4.94(24) \times 10^{-1}$	$4.94(24) \times 10^{-1}$	$6.24(33) \times 10^{-4}$	$6.24(33) \times 10^{-4}$	$6.24(33) \times 10^{-4}$
${}^4P \rightarrow {}^{12}S$	$3.31(20) \times 10^{-1}$	$3.31(20) \times 10^{-1}$	$3.31(20) \times 10^{-1}$	$4.44(32) \times 10^{-4}$	$4.44(32) \times 10^{-4}$	$4.44(32) \times 10^{-4}$
${}^5S \rightarrow {}^5P$	$9.958\,35(81) \times 10^2$	$9.958\,42(80) \times 10^2$	$9.959\,02(80) \times 10^2$	$3.439\,52(14) \times 10^{-2}$	$3.439\,48(13) \times 10^{-2}$	$3.438\,97(13) \times 10^{-2}$
${}^5S \rightarrow {}^6P$	8.191 1(78)	8.191 4(75)	8.190 3(81)	$1.650\,18(40) \times 10^{-3}$	$1.650\,13(40) \times 10^{-3}$	$1.649\,33(40) \times 10^{-3}$
${}^5S \rightarrow {}^7P$	1.061 6(44)	1.061 5(44)	1.060 9(40)	$3.818\,9(40) \times 10^{-4}$	$3.818\,7(40) \times 10^{-4}$	$3.816\,3(40) \times 10^{-4}$
${}^5S \rightarrow {}^8P$	$2.930\,4(78) \times 10^{-1}$	$2.930\,3(81) \times 10^{-1}$	$2.926\,7(82) \times 10^{-1}$	$1.422\,4(70) \times 10^{-4}$	$1.422\,3(70) \times 10^{-4}$	$1.421\,1(60) \times 10^{-4}$
${}^5S \rightarrow {}^9P$	$1.189\,7(93) \times 10^{-1}$	$1.189\,6(94) \times 10^{-1}$	$1.187\,7(93) \times 10^{-1}$	$6.903(30) \times 10^{-5}$	$6.902(30) \times 10^{-5}$	$6.898(20) \times 10^{-5}$
${}^5S \rightarrow {}^{10}P$	$5.997(43) \times 10^{-2}$	$5.996(43) \times 10^{-2}$	$5.986(43) \times 10^{-2}$	$3.878(70) \times 10^{-5}$	$3.878(70) \times 10^{-5}$	$3.874(70) \times 10^{-5}$
${}^5P \rightarrow {}^6S$	$8.540\,99(35) \times 10^2$	$8.540\,94(35) \times 10^2$	$8.540\,39(34) \times 10^2$	$1.922\,20(30) \times 10^{-2}$	$1.922\,44(28) \times 10^{-2}$	$1.924\,54(32) \times 10^{-2}$
${}^5P \rightarrow {}^7S$	$4.32(14) \times 10^{-2}$	$4.11(14) \times 10^{-2}$	$2.33(14) \times 10^{-2}$	$4.00(10) \times 10^{-6}$	$3.82(10) \times 10^{-6}$	$2.20(10) \times 10^{-6}$
${}^5P \rightarrow {}^8S$	$2.082\,4(53) \times 10^1$	$2.081\,4(50) \times 10^1$	$2.068\,0(53) \times 10^1$	$3.168\,2(72) \times 10^{-3}$	$3.167\,2(69) \times 10^{-3}$	$3.152\,4(75) \times 10^{-3}$
${}^5P \rightarrow {}^9S$	8.860(91)	8.860(91)	8.862(92)	$2.068\,3(73) \times 10^{-3}$	$2.068\,4(73) \times 10^{-3}$	$2.069\,4(74) \times 10^{-3}$
${}^5P \rightarrow {}^{10}S$	3.941(29)	3.941(29)	3.942(29)	$1.191\,0(92) \times 10^{-3}$	$1.191\,0(92) \times 10^{-3}$	$1.191\,5(92) \times 10^{-3}$
${}^5P \rightarrow {}^{11}S$	2.074(76)	2.074(76)	2.074(76)	$7.32(41) \times 10^{-4}$	$7.32(41) \times 10^{-4}$	$7.32(41) \times 10^{-4}$
${}^5P \rightarrow {}^{12}S$	1.264(51)	1.264(51)	1.264(51)	$4.95(42) \times 10^{-4}$	$4.95(42) \times 10^{-4}$	$4.95(42) \times 10^{-4}$

TABLE VI. (Continued.)

Transition	$ \mu_{ij}^L ^2(^{10}\text{B})$	$ \mu_{ij}^L ^2(^{11}\text{B})$	$ \mu_{ij}^L ^2(^{\infty}\text{B})$	$ \mu_{ij}^V ^2(^{10}\text{B})$	$ \mu_{ij}^V ^2(^{11}\text{B})$	$ \mu_{ij}^V ^2(^{\infty}\text{B})$
$6^2S \rightarrow 6^2P$	$1.80399(40) \times 10^3$	$1.80427(38) \times 10^3$	$1.80697(35) \times 10^3$	$2.31575(21) \times 10^{-2}$	$2.31579(20) \times 10^{-2}$	$2.31605(16) \times 10^{-2}$
$6^2S \rightarrow 7^2P$	$3.261(16) \times 10^1$	$3.260(16) \times 10^1$	$3.253(17) \times 10^1$	$2.2752(17) \times 10^{-3}$	$2.2748(18) \times 10^{-3}$	$2.2707(18) \times 10^{-3}$
$6^2S \rightarrow 8^2P$	5.853(37)	5.852(37)	5.843(37)	$7.519(27) \times 10^{-4}$	$7.517(27) \times 10^{-4}$	$7.497(30) \times 10^{-4}$
$6^2S \rightarrow 9^2P$	2.016(18)	2.016(18)	2.012(17)	$3.610(16) \times 10^{-4}$	$3.609(16) \times 10^{-4}$	$3.598(16) \times 10^{-4}$
$6^2S \rightarrow 10^2P$	$9.651(94) \times 10^{-1}$	$9.649(94) \times 10^{-1}$	$9.628(91) \times 10^{-1}$	$2.078(21) \times 10^{-4}$	$2.077(21) \times 10^{-4}$	$2.068(23) \times 10^{-4}$
$6^2P \rightarrow 7^2S$	$1.89340(99) \times 10^3$	$1.8933(12) \times 10^3$	$1.8909(17) \times 10^3$	$2.9136(29) \times 10^{-3}$	$2.9190(30) \times 10^{-3}$	$2.9729(36) \times 10^{-3}$
$6^2P \rightarrow 8^2S$	$5.085(14) \times 10^2$	$5.079(14) \times 10^2$	$5.020(13) \times 10^2$	$8.1775(47) \times 10^{-3}$	$8.1716(49) \times 10^{-3}$	$8.1134(53) \times 10^{-3}$
$6^2P \rightarrow 9^2S$	$7.053(91) \times 10^1$	$7.053(91) \times 10^1$	$7.053(91) \times 10^1$	$3.433(15) \times 10^{-3}$	$3.433(15) \times 10^{-3}$	$3.434(15) \times 10^{-3}$
$6^2P \rightarrow 10^2S$	$1.974(40) \times 10^1$	$1.974(40) \times 10^1$	$1.975(40) \times 10^1$	$1.633(14) \times 10^{-3}$	$1.633(14) \times 10^{-3}$	$1.633(14) \times 10^{-3}$
$6^2P \rightarrow 11^2S$	8.30(25)	8.30(25)	8.30(24)	$9.21(42) \times 10^{-4}$	$9.21(42) \times 10^{-4}$	$9.21(42) \times 10^{-4}$
$6^2P \rightarrow 12^2S$	4.58(13)	4.57(13)	4.58(14)	$5.83(44) \times 10^{-4}$	$5.83(44) \times 10^{-4}$	$5.83(44) \times 10^{-4}$
$7^2S \rightarrow 7^2P$	$7.919(11) \times 10^2$	$7.925(10) \times 10^2$	$8.000(13) \times 10^2$	$9.858(16) \times 10^{-3}$	$9.863(17) \times 10^{-3}$	$9.913(16) \times 10^{-3}$
$7^2S \rightarrow 8^2P$	$6.671(23) \times 10^1$	$6.671(24) \times 10^1$	$6.672(27) \times 10^1$	$2.81448(60) \times 10^{-3}$	$2.81558(50) \times 10^{-3}$	$2.82591(60) \times 10^{-3}$
$7^2S \rightarrow 9^2P$	$1.889(12) \times 10^1$	$1.889(12) \times 10^1$	$1.895(12) \times 10^1$	$1.3567(44) \times 10^{-3}$	$1.3572(44) \times 10^{-3}$	$1.3627(46) \times 10^{-3}$
$7^2S \rightarrow 10^2P$	8.352(44)	8.355(44)	8.390(50)	$8.001(75) \times 10^{-4}$	$8.006(73) \times 10^{-4}$	$8.037(74) \times 10^{-4}$
$7^2P \rightarrow 9^2S$	$2.148(12) \times 10^3$	$2.148(12) \times 10^3$	$2.143(11) \times 10^3$	$1.03300(17) \times 10^{-2}$	$1.03290(16) \times 10^{-2}$	$1.03184(17) \times 10^{-2}$
$7^2P \rightarrow 10^2S$	$1.420(56) \times 10^2$	$1.420(56) \times 10^2$	$1.420(56) \times 10^2$	$2.742(35) \times 10^{-3}$	$2.742(35) \times 10^{-3}$	$2.741(35) \times 10^{-3}$
$7^2P \rightarrow 11^2S$	$3.64(35) \times 10^1$	$3.64(35) \times 10^1$	$3.64(35) \times 10^1$	$1.278(62) \times 10^{-3}$	$1.278(62) \times 10^{-3}$	$1.278(62) \times 10^{-3}$
$7^2P \rightarrow 12^2S$	$1.622(22) \times 10^1$	$1.622(22) \times 10^1$	$1.621(22) \times 10^1$	$7.49(39) \times 10^{-4}$	$7.55(32) \times 10^{-4}$	$7.55(32) \times 10^{-4}$
$8^2S \rightarrow 7^2P$	$5.3598(67) \times 10^3$	$5.3582(65) \times 10^3$	$5.3402(53) \times 10^3$	$3.0465(35) \times 10^{-3}$	$3.0420(34) \times 10^{-3}$	$2.9988(31) \times 10^{-3}$
$8^2S \rightarrow 8^2P$	$5.067(63) \times 10^1$	$5.069(65) \times 10^1$	$5.120(62) \times 10^1$	$7.171(89) \times 10^{-4}$	$7.182(91) \times 10^{-4}$	$7.29(11) \times 10^{-4}$
$8^2S \rightarrow 9^2P$	$1.379(70) \times 10^1$	$1.379(70) \times 10^1$	$1.380(70) \times 10^1$	$4.646(51) \times 10^{-4}$	$4.651(51) \times 10^{-4}$	$4.702(54) \times 10^{-4}$
$8^2S \rightarrow 10^2P$	5.98(14)	5.98(14)	6.00(14)	$3.0491(30) \times 10^{-4}$	$3.0524(30) \times 10^{-4}$	$3.0847(40) \times 10^{-4}$
$8^2P \rightarrow 10^2S$	$4.371(25) \times 10^3$	$4.370(25) \times 10^3$	$4.366(24) \times 10^3$	$8.765(47) \times 10^{-3}$	$8.765(47) \times 10^{-3}$	$8.759(47) \times 10^{-3}$
$8^2P \rightarrow 11^2S$	$2.27(54) \times 10^2$	$2.27(54) \times 10^2$	$2.27(54) \times 10^2$	$2.18(14) \times 10^{-3}$	$2.18(14) \times 10^{-3}$	$2.18(13) \times 10^{-3}$
$8^2P \rightarrow 12^2S$	$7.09(43) \times 10^1$	$7.09(43) \times 10^1$	$7.09(43) \times 10^1$	$1.068(55) \times 10^{-3}$	$1.068(54) \times 10^{-3}$	$1.067(54) \times 10^{-3}$
$9^2S \rightarrow 8^2P$	$1.0323(53) \times 10^4$	$1.0323(53) \times 10^4$	$1.0319(53) \times 10^4$	$6.435(34) \times 10^{-3}$	$6.433(34) \times 10^{-3}$	$6.417(34) \times 10^{-3}$
$9^2S \rightarrow 9^2P$	$4.8(27) \times 10^{-1}$	$4.8(27) \times 10^{-1}$	$4.4(25) \times 10^{-1}$	$5.5(60) \times 10^{-7}$	$5.5(60) \times 10^{-7}$	$3.5(70) \times 10^{-7}$
$9^2S \rightarrow 10^2P$	$2.9(47) \times 10^{-1}$	$3.0(47) \times 10^{-1}$	$3.0(47) \times 10^{-1}$	$1.28(30) \times 10^{-5}$	$1.30(32) \times 10^{-5}$	$1.33(33) \times 10^{-5}$
$9^2P \rightarrow 11^2S$	$7.83(49) \times 10^3$	$7.83(49) \times 10^3$	$7.83(49) \times 10^3$	$7.146(47) \times 10^{-3}$	$7.143(44) \times 10^{-3}$	$7.140(46) \times 10^{-3}$
$9^2P \rightarrow 12^2S$	$3.9(13) \times 10^2$	$3.9(13) \times 10^2$	$3.9(12) \times 10^2$	$1.72(23) \times 10^{-3}$	$1.72(23) \times 10^{-3}$	$1.72(23) \times 10^{-3}$
$10^2S \rightarrow 9^2P$	$1.692(35) \times 10^4$	$1.687(40) \times 10^4$	$1.687(40) \times 10^4$	$5.91(10) \times 10^{-3}$	$5.91(10) \times 10^{-3}$	$5.90(10) \times 10^{-3}$
$10^2S \rightarrow 10^2P$	$2.00(82) \times 10^1$	$2.00(82) \times 10^1$	$1.98(81) \times 10^1$	$4.5(21) \times 10^{-5}$	$4.5(21) \times 10^{-5}$	$4.5(21) \times 10^{-5}$
$10^2P \rightarrow 12^2S$	$1.38(20) \times 10^4$	$1.38(20) \times 10^4$	$1.38(20) \times 10^4$	$6.20(52) \times 10^{-3}$	$6.20(52) \times 10^{-3}$	$6.19(52) \times 10^{-3}$
$11^2S \rightarrow 10^2P$	$2.56(23) \times 10^4$	$2.56(23) \times 10^4$	$2.56(23) \times 10^4$	$5.07(36) \times 10^{-3}$	$5.07(36) \times 10^{-3}$	$5.06(36) \times 10^{-3}$

One can also observe two dark spots in Figs. 1(a) and 1(b) that correspond to the  $4^2P \rightarrow 7^2S$  and  $5^2P \rightarrow 3^2S$  transitions. The last one corresponds to the smallest calculated value ( $\sim 3 \times 10^{-5}$  or  $\sim 3 \times 10^{-7}$ , depending on the gauge used) among all  $f$  values found in Table VII. Because these values have such small magnitudes, their relative uncertainties are large. Yet, because the data are consistent across the gauges ( $L$  and  $V$ ) we strongly believe that the exact oscillator strength for for both  $4^2P \rightarrow 7^2S$  and  $5^2P \rightarrow 3^2S$  transitions is indeed very small.

In Figs. 1(c) and 1(d), the relative isotopic shifts of the oscillator strengths (RIS of  $f$ ) are shown for all studied transitions. They are calculated in the length and velocity gauges as  $[f(^{10}\text{B}) - f(^{11}\text{B})]/f(^{11}\text{B})$ . The plots show that, as expected, the oscillator strengths are almost identical for the two boron isotopes, with some exceptions.

Table VIII shows all transitions for which the absolute values of the RIS are larger than  $2.5 \times 10^{-3}$ . One can see that the largest RIS values correspond to the  $4^2P \rightarrow 7^2S$  and  $5^2P \rightarrow 7^2S$  transitions. Both of these values are close to 5% and there is a reasonably good agreement (within estimated

uncertainties) between the values computed in the length and velocity gauge, which gives confidence that this is not merely a numerical artifact. Such a significant magnitude of the RIS makes it potentially detectable in future experiments with different boron isotopes.

It should be noted that the estimated uncertainties for the RIS values given in Table VIII are considerably smaller than the root-mean-square errors in which the uncertainties in  $f$  values for the two isotopes are uncorrelated. This is because the errors in the oscillator strength are correlated in our calculations, where we use the same ECG basis sets for the same states of different isotopes. Thus, when estimating the uncertainties of the RIS we looked specifically at the convergence patterns of this quantity as we increased the basis size.

The higher sensitivity (in relative terms) of the  $4^2P \rightarrow 7^2S$  and  $5^2P \rightarrow 7^2S$  transition to the isotopic substitution may be related to two facts. First, the oscillator strengths themselves for these transitions are rather small [hence, the dark spots in Figs. 1(a) and 1(b)]. Second, as it was previously mentioned, there is an admixture in the configuration composition of the  $7^2S$  state. Apparently, the transition matrix

TABLE VII. Nonrelativistic absorption oscillator strengths obtained using the length ( $f_{if}^L$ ) and velocity ( $f_{if}^V$ ) formalisms for the transitions involving  ${}^2S$  and  ${}^2P$  states of the boron atom. The oscillator strength uncertainties (numbers in parentheses) are calculated as the root mean squares of the uncertainties of  $|\mu_{if}^L|^2$  or  $|\mu_{if}^V|^2$  and  $\Delta E$ , where  $\Delta E$  is the difference between the nonrelativistic total energies of the initial ( $i$ ) and final ( $f$ ) states.

Transition	$f_{if}^L({}^{10}B)$	$f_{if}^V({}^{10}B)$	$f_{if}^L({}^{10}B)$	$f_{if}^V({}^{10}B)$	$f_{if}^L(\infty B)$	$f_{if}^V(\infty B)$
${}^2P \rightarrow {}^3S$	$7.869\,32(12) \times 10^{-2}$	$7.869\,377(42) \times 10^{-2}$	$7.869\,32(12) \times 10^{-2}$	$7.869\,368(42) \times 10^{-2}$	$7.869\,25(12) \times 10^{-2}$	$7.869\,350(42) \times 10^{-2}$
${}^2P \rightarrow {}^3S$	Ref. [42]				$7.83(23) \times 10^{-2}$	
${}^2P \rightarrow {}^3S$	Ref. [51]				$8.03 \times 10^{-2}$	$7.95 \times 10^{-2}$
${}^2P \rightarrow {}^3S$	Ref. [52]				$7.87 \times 10^{-2}$	$7.61 \times 10^{-2}$
${}^2P \rightarrow {}^4S$	$1.645\,59(20) \times 10^{-2}$	$1.645\,411(20) \times 10^{-2}$	$1.645\,54(20) \times 10^{-2}$	$1.645\,355(20) \times 10^{-2}$	$1.644\,98(20) \times 10^{-2}$	$1.644\,793(20) \times 10^{-2}$
${}^2P \rightarrow {}^4S$	Ref. [42]				$1.54(15) \times 10^{-2}$	
${}^2P \rightarrow {}^4S$	Ref. [51]				$1.62 \times 10^{-2}$	$1.65 \times 10^{-2}$
${}^2P \rightarrow {}^4S$	Ref. [52]				$1.63 \times 10^{-2}$	$1.57 \times 10^{-2}$
${}^2P \rightarrow {}^5S$	$1.103\,88(12) \times 10^{-2}$	$1.103\,89(17) \times 10^{-2}$	$1.103\,72(12) \times 10^{-2}$	$1.103\,74(17) \times 10^{-2}$	$1.102\,21(12) \times 10^{-2}$	$1.102\,22(17) \times 10^{-2}$
${}^2P \rightarrow {}^5S$	Ref. [42]				$8.2(2\,1) \times 10^{-3}$	
${}^2P \rightarrow {}^5S$	Ref. [51]				$1.17 \times 10^{-2}$	$1.22 \times 10^{-2}$
${}^2P \rightarrow {}^5S$	Ref. [52]				$1.06 \times 10^{-2}$	$1.02 \times 10^{-2}$
${}^2P \rightarrow {}^6S$	$1.681\,87(38) \times 10^{-2}$	$1.681\,86(36) \times 10^{-2}$	$1.681\,13(38) \times 10^{-2}$	$1.681\,15(36) \times 10^{-2}$	$1.674\,00(38) \times 10^{-2}$	$1.673\,96(36) \times 10^{-2}$
${}^2P \rightarrow {}^6S$	Ref. [42]				$1.08(54) \times 10^{-2}$	
${}^2P \rightarrow {}^6S$	Ref. [52]				$1.48 \times 10^{-2}$	$1.43 \times 10^{-2}$
${}^2P \rightarrow {}^7S$	$3.821\,3(20) \times 10^{-2}$	$3.821\,5(37) \times 10^{-2}$	$3.821\,6(20) \times 10^{-2}$	$3.821\,7(37) \times 10^{-2}$	$3.824\,8(20) \times 10^{-2}$	$3.823\,1(37) \times 10^{-2}$
${}^2P \rightarrow {}^7S$	Ref. [42]				$1.64(41) \times 10^{-2}$	
${}^2P \rightarrow {}^7S$	Ref. [52]				$3.53 \times 10^{-2}$	$3.41 \times 10^{-2}$
${}^2P \rightarrow {}^8S$	$1.260\,97(70) \times 10^{-2}$	$1.261\,23(47) \times 10^{-2}$	$1.263\,00(70) \times 10^{-2}$	$1.263\,25(47) \times 10^{-2}$	$1.283\,49(70) \times 10^{-2}$	$1.283\,67(47) \times 10^{-2}$
${}^2P \rightarrow {}^8S$	Ref. [42]				$7.4(1\,9) \times 10^{-3}$	
${}^2P \rightarrow {}^8S$	Ref. [52]				$1.78 \times 10^{-2}$	$1.72 \times 10^{-2}$
${}^2P \rightarrow {}^9S$	$1.553\,9(16) \times 10^{-3}$	$1.553\,7(16) \times 10^{-3}$	$1.556\,6(16) \times 10^{-3}$	$1.556\,4(16) \times 10^{-3}$	$1.583\,9(16) \times 10^{-3}$	$1.583\,6(16) \times 10^{-3}$
${}^2P \rightarrow {}^9S$	Ref. [42]				$1.00(25) \times 10^{-2}$	
${}^2P \rightarrow {}^9S$	Ref. [52]				$2.38 \times 10^{-3}$	$2.3 \times 10^{-3}$
${}^2P \rightarrow {}^{10}S$	$3.404\,(27) \times 10^{-4}$	$3.402\,(26) \times 10^{-4}$	$3.410\,(27) \times 10^{-4}$	$3.408\,(26) \times 10^{-4}$	$3.474\,(27) \times 10^{-4}$	$3.472\,(26) \times 10^{-4}$
${}^2P \rightarrow {}^{11}S$	$1.091\,(35) \times 10^{-4}$	$1.090\,(35) \times 10^{-4}$	$1.094\,(35) \times 10^{-4}$	$1.092\,(35) \times 10^{-4}$	$1.119\,(35) \times 10^{-4}$	$1.116\,(35) \times 10^{-4}$
${}^2P \rightarrow {}^{12}S$	$4.53(19) \times 10^{-5}$	$4.51(17) \times 10^{-5}$	$4.54(19) \times 10^{-5}$	$4.52(17) \times 10^{-5}$	$4.65(19) \times 10^{-5}$	$4.63(17) \times 10^{-5}$
${}^3S \rightarrow {}^3P$	1.051 8577(26)	1.051 882(13)	1.051 8573(26)	1.051 876(13)	1.051 8536(26)	1.051 827(15)
${}^3S \rightarrow {}^3P$	Ref. [42]				1.05(11)	
${}^3S \rightarrow {}^3P$	Ref. [51]				1.07	1.08
${}^3S \rightarrow {}^3P$	Ref. [52]				1.05	1.04
${}^3S \rightarrow {}^4P$	$2.580\,1(10) \times 10^{-3}$	$2.579\,25(45) \times 10^{-3}$	$2.580\,5(10) \times 10^{-3}$	$2.579\,66(45) \times 10^{-3}$	$2.584\,5(10) \times 10^{-3}$	$2.583\,76(45) \times 10^{-3}$
${}^3S \rightarrow {}^4P$	Ref. [42]				$3.21(80) \times 10^{-3}$	
${}^3S \rightarrow {}^4P$	Ref. [52]				$2.67 \times 10^{-3}$	$2.52 \times 10^{-3}$
${}^3S \rightarrow {}^5P$	$1.202\,(50) \times 10^{-6}$	$1.150\,(10) \times 10^{-6}$	$1.196\,(50) \times 10^{-6}$	$1.143\,(10) \times 10^{-6}$	$1.132\,(50) \times 10^{-6}$	$1.083\,(10) \times 10^{-6}$
${}^3S \rightarrow {}^6P$	$9.160\,(27) \times 10^{-5}$	$9.128\,4(70) \times 10^{-5}$	$9.155\,(27) \times 10^{-5}$	$9.124\,4(70) \times 10^{-5}$	$9.113\,(27) \times 10^{-5}$	$9.085\,0(60) \times 10^{-5}$
${}^3S \rightarrow {}^7P$	$1.138\,4(28) \times 10^{-4}$	$1.138\,1(19) \times 10^{-4}$	$1.138\,0(28) \times 10^{-4}$	$1.137\,7(19) \times 10^{-4}$	$1.134\,1(28) \times 10^{-4}$	$1.134\,1(19) \times 10^{-4}$
${}^3S \rightarrow {}^8P$	$1.015\,2(65) \times 10^{-4}$	$1.016\,4(67) \times 10^{-4}$	$1.014\,9(65) \times 10^{-4}$	$1.016\,1(67) \times 10^{-4}$	$1.011\,9(65) \times 10^{-4}$	$1.013\,4(67) \times 10^{-4}$
${}^3S \rightarrow {}^9P$	$8.224\,(44) \times 10^{-5}$	$8.240\,(25) \times 10^{-5}$	$8.222\,(44) \times 10^{-5}$	$8.237\,(25) \times 10^{-5}$	$8.196\,(44) \times 10^{-5}$	$8.214\,(25) \times 10^{-5}$
${}^3S \rightarrow {}^{10}P$	$6.544\,(39) \times 10^{-5}$	$6.554\,(11) \times 10^{-5}$	$6.542\,(39) \times 10^{-5}$	$6.553\,(11) \times 10^{-5}$	$6.524\,(39) \times 10^{-5}$	$6.537\,(12) \times 10^{-5}$
${}^3P \rightarrow {}^4S$	$2.014\,6878(43) \times 10^{-1}$	$2.014\,646(23) \times 10^{-1}$	$2.014\,6987(43) \times 10^{-1}$	$2.014\,654(23) \times 10^{-1}$	$2.014\,7281(43) \times 10^{-1}$	$2.014\,727(23) \times 10^{-1}$
${}^3P \rightarrow {}^4S$	Ref. [42]				$2.03(20) \times 10^{-1}$	
${}^3P \rightarrow {}^4S$	Ref. [51]				$2.04 \times 10^{-1}$	$2.06 \times 10^{-1}$
${}^3P \rightarrow {}^4S$	Ref. [52]				$2.02 \times 10^{-1}$	$2.00 \times 10^{-1}$
${}^3P \rightarrow {}^5S$	$2.044\,71(45) \times 10^{-2}$	$2.043\,93(10) \times 10^{-2}$	$2.044\,71(45) \times 10^{-2}$	$2.043\,94(10) \times 10^{-2}$	$2.044\,76(45) \times 10^{-2}$	$2.043\,969(99) \times 10^{-2}$
${}^3P \rightarrow {}^5S$	Ref. [42]				$2.07(21) \times 10^{-2}$	
${}^3P \rightarrow {}^5S$	Ref. [52]				$2.05 \times 10^{-2}$	$2.03 \times 10^{-2}$
${}^3P \rightarrow {}^6S$	$5.904\,0(62) \times 10^{-3}$	$5.912\,4(20) \times 10^{-3}$	$5.904\,9(62) \times 10^{-3}$	$5.913\,3(20) \times 10^{-3}$	$5.914\,4(62) \times 10^{-3}$	$5.922\,5(23) \times 10^{-3}$
${}^3P \rightarrow {}^6S$	Ref. [42]				$6.7(1\,7) \times 10^{-3}$	
${}^3P \rightarrow {}^6S$	Ref. [52]				$6.14 \times 10^{-3}$	$6.14 \times 10^{-3}$
${}^3P \rightarrow {}^7S$	$2.624\,(13) \times 10^{-4}$	$2.622\,5(92) \times 10^{-4}$	$2.636\,(13) \times 10^{-4}$	$2.634\,5(89) \times 10^{-4}$	$2.760\,(13) \times 10^{-4}$	$2.760\,4(97) \times 10^{-4}$
${}^3P \rightarrow {}^8S$	$1.450\,6(39) \times 10^{-3}$	$1.452\,5(29) \times 10^{-3}$	$1.449\,2(39) \times 10^{-3}$	$1.451\,1(30) \times 10^{-3}$	$1.436\,4(39) \times 10^{-3}$	$1.438\,4(32) \times 10^{-3}$
${}^3P \rightarrow {}^8S$	Ref. [42]				$3.22(81) \times 10^{-3}$	
${}^3P \rightarrow {}^8S$	Ref. [52]				$6.78 \times 10^{-4}$	$6.29 \times 10^{-4}$
${}^3P \rightarrow {}^9S$	$1.570\,2(58) \times 10^{-3}$	$1.571\,2(58) \times 10^{-3}$	$1.570\,1(58) \times 10^{-3}$	$1.571\,2(58) \times 10^{-3}$	$1.569\,0(58) \times 10^{-3}$	$1.570\,4(60) \times 10^{-3}$

TABLE VII. (Continued.)

Transition	$f_{if}^L(^{10}\text{B})$	$f_{if}^V(^{10}\text{B})$	$f_{if}^L(^{10}\text{B})$	$f_{if}^V(^{10}\text{B})$	$f_{if}^L(^{\infty}\text{B})$	$f_{if}^V(^{\infty}\text{B})$
$3^2P \rightarrow 9^2S$	Ref. [42]				$1.57(39) \times 10^{-3}$	
$3^2P \rightarrow 9^2S$	Ref. [52]				$9.57 \times 10^{-4}$	$8.76 \times 10^{-4}$
$3^2P \rightarrow 10^2S$	$1.091(11) \times 10^{-3}$	$1.090(12) \times 10^{-3}$	$1.091(11) \times 10^{-3}$	$1.090(12) \times 10^{-3}$	$1.090(11) \times 10^{-3}$	$1.090(12) \times 10^{-3}$
$3^2P \rightarrow 10^2S$	Ref. [52]				$1.48 \times 10^{-3}$	$1.42 \times 10^{-3}$
$3^2P \rightarrow 11^2S$	$7.50(33) \times 10^{-4}$	$7.48(36) \times 10^{-4}$	$7.50(33) \times 10^{-4}$	$7.48(36) \times 10^{-4}$	$7.50(33) \times 10^{-4}$	$7.48(36) \times 10^{-4}$
$3^2P \rightarrow 12^2S$	$5.47(33) \times 10^{-4}$	$5.42(39) \times 10^{-4}$	$5.47(33) \times 10^{-4}$	$5.42(39) \times 10^{-4}$	$5.46(33) \times 10^{-4}$	$5.42(39) \times 10^{-4}$
$4^2S \rightarrow 4^2P$	1.536 453(12)	1.536 517(39)	1.536 451(12)	1.536 501(39)	1.536 436(12)	1.536 344(45)
$4^2S \rightarrow 4^2P$	Ref. [42]				1.55(16)	
$4^2S \rightarrow 5^2P$	$1.64032(64) \times 10^{-2}$	$1.63923(32) \times 10^{-2}$	$1.64041(65) \times 10^{-2}$	$1.63927(32) \times 10^{-2}$	$1.64128(72) \times 10^{-2}$	$1.63984(30) \times 10^{-2}$
$4^2S \rightarrow 6^2P$	$1.7483(52) \times 10^{-3}$	$1.75471(77) \times 10^{-3}$	$1.7486(52) \times 10^{-3}$	$1.75478(85) \times 10^{-3}$	$1.7507(52) \times 10^{-3}$	$1.75625(86) \times 10^{-3}$
$4^2S \rightarrow 7^2P$	$3.617(10) \times 10^{-4}$	$3.6150(99) \times 10^{-4}$	$3.6181(96) \times 10^{-4}$	$3.6155(98) \times 10^{-4}$	$3.624(10) \times 10^{-4}$	$3.6205(95) \times 10^{-4}$
$4^2S \rightarrow 8^2P$	$1.0398(79) \times 10^{-4}$	$1.0283(79) \times 10^{-4}$	$1.0401(79) \times 10^{-4}$	$1.0281(83) \times 10^{-4}$	$1.0428(78) \times 10^{-4}$	$1.0303(84) \times 10^{-4}$
$4^2S \rightarrow 9^2P$	$3.818(39) \times 10^{-5}$	$3.767(46) \times 10^{-5}$	$3.820(38) \times 10^{-5}$	$3.758(57) \times 10^{-5}$	$3.834(36) \times 10^{-5}$	$3.774(50) \times 10^{-5}$
$4^2S \rightarrow 10^2P$	$1.619(58) \times 10^{-5}$	$1.52(12) \times 10^{-5}$	$1.618(59) \times 10^{-5}$	$1.52(12) \times 10^{-5}$	$1.624(60) \times 10^{-5}$	$1.53(11) \times 10^{-5}$
$4^2P \rightarrow 5^2S$	$3.325289(73) \times 10^{-1}$	$3.325138(73) \times 10^{-1}$	$3.325295(73) \times 10^{-1}$	$3.325131(73) \times 10^{-1}$	$3.325350(74) \times 10^{-1}$	$3.325171(74) \times 10^{-1}$
$4^2P \rightarrow 5^2S$	Ref. [42]				$3.35(34) \times 10^{-1}$	
$4^2P \rightarrow 5^2S$	Ref. [52]				$3.33 \times 10^{-1}$	$3.32 \times 10^{-1}$
$4^2P \rightarrow 6^2S$	$2.3100(20) \times 10^{-2}$	$2.30822(82) \times 10^{-2}$	$2.3105(20) \times 10^{-2}$	$2.30868(85) \times 10^{-2}$	$2.3155(21) \times 10^{-2}$	$2.31357(82) \times 10^{-2}$
$4^2P \rightarrow 6^2S$	Ref. [42]				$2.77(28) \times 10^{-2}$	
$4^2P \rightarrow 6^2S$	Ref. [52]				$2.44 \times 10^{-2}$	$2.44 \times 10^{-2}$
$4^2P \rightarrow 7^2S$	$9.11(50) \times 10^{-6}$	$9.29(37) \times 10^{-6}$	$9.55(51) \times 10^{-6}$	$9.71(36) \times 10^{-6}$	$1.446(56) \times 10^{-5}$	$1.460(41) \times 10^{-5}$
$4^2P \rightarrow 8^2S$	$7.0273(32) \times 10^{-3}$	$7.019(13) \times 10^{-3}$	$7.0237(32) \times 10^{-3}$	$7.015(13) \times 10^{-3}$	$6.9861(36) \times 10^{-3}$	$6.978(16) \times 10^{-3}$
$4^2P \rightarrow 8^2S$	Ref. [42]				$8.98(90) \times 10^{-3}$	
$4^2P \rightarrow 8^2S$	Ref. [52]				$5.32 \times 10^{-4}$	$4.85 \times 10^{-4}$
$4^2P \rightarrow 9^2S$	$5.155(17) \times 10^{-3}$	$5.162(20) \times 10^{-3}$	$5.155(17) \times 10^{-3}$	$5.162(20) \times 10^{-3}$	$5.157(17) \times 10^{-3}$	$5.164(20) \times 10^{-3}$
$4^2P \rightarrow 9^2S$	Ref. [42]				$3.03(76) \times 10^{-3}$	
$4^2P \rightarrow 9^2S$	Ref. [52]				$5.36 \times 10^{-3}$	$5.17 \times 10^{-3}$
$4^2P \rightarrow 10^2S$	$3.088(33) \times 10^{-3}$	$3.089(34) \times 10^{-3}$	$3.088(33) \times 10^{-3}$	$3.090(34) \times 10^{-3}$	$3.089(34) \times 10^{-3}$	$3.091(34) \times 10^{-3}$
$4^2P \rightarrow 10^2S$	Ref. [52]				$5.03 \times 10^{-3}$	$4.92 \times 10^{-3}$
$4^2P \rightarrow 11^2S$	$1.954(94) \times 10^{-3}$	$1.95(10) \times 10^{-3}$	$1.954(94) \times 10^{-3}$	$1.95(10) \times 10^{-3}$	$1.954(94) \times 10^{-3}$	$1.95(10) \times 10^{-3}$
$4^2P \rightarrow 12^2S$	$1.349(83) \times 10^{-3}$	$1.344(96) \times 10^{-3}$	$1.349(83) \times 10^{-3}$	$1.344(96) \times 10^{-3}$	$1.349(83) \times 10^{-3}$	$1.344(96) \times 10^{-3}$
$5^2S \rightarrow 5^2P$	1.950 69(16)	1.950 989(83)	1.950 70(16)	1.950 968(78)	1.950 80(16)	1.950 701(77)
$5^2S \rightarrow 6^2P$	$3.8781(37) \times 10^{-2}$	$3.87274(98) \times 10^{-2}$	$3.8782(36) \times 10^{-2}$	$3.87262(93) \times 10^{-2}$	$3.8777(38) \times 10^{-2}$	$3.8707(10) \times 10^{-2}$
$5^2S \rightarrow 7^2P$	$6.713(28) \times 10^{-3}$	$6.7104(72) \times 10^{-3}$	$6.712(28) \times 10^{-3}$	$6.7100(70) \times 10^{-3}$	$6.709(26) \times 10^{-3}$	$6.7057(64) \times 10^{-3}$
$5^2S \rightarrow 8^2P$	$2.1438(58) \times 10^{-3}$	$2.160(10) \times 10^{-3}$	$2.1437(60) \times 10^{-3}$	$2.160(1) \times 10^{-3}$	$2.1411(61) \times 10^{-3}$	$2.1583(96) \times 10^{-3}$
$5^2S \rightarrow 9^2P$	$9.494(75) \times 10^{-4}$	$9.611(37) \times 10^{-4}$	$9.493(76) \times 10^{-4}$	$9.610(37) \times 10^{-4}$	$9.479(75) \times 10^{-4}$	$9.604(33) \times 10^{-4}$
$5^2S \rightarrow 10^2P$	$5.066(37) \times 10^{-4}$	$5.101(88) \times 10^{-4}$	$5.065(38) \times 10^{-4}$	$5.101(88) \times 10^{-4}$	$5.056(38) \times 10^{-4}$	$5.096(87) \times 10^{-4}$
$5^2P \rightarrow 6^2S$	$4.50237(81) \times 10^{-1}$	$4.5017(11) \times 10^{-1}$	$4.50263(81) \times 10^{-1}$	$4.5020(10) \times 10^{-1}$	$4.50514(81) \times 10^{-1}$	$4.5041(11) \times 10^{-1}$
$5^2P \rightarrow 7^2S$	$4.59(15) \times 10^{-5}$	$4.648(94) \times 10^{-5}$	$4.37(15) \times 10^{-5}$	$4.434(93) \times 10^{-5}$	$2.48(15) \times 10^{-5}$	$2.557(82) \times 10^{-5}$
$5^2P \rightarrow 8^2S$	$2.8546(75) \times 10^{-2}$	$2.8533(67) \times 10^{-2}$	$2.8534(70) \times 10^{-2}$	$2.8522(64) \times 10^{-2}$	$2.8366(74) \times 10^{-2}$	$2.8373(70) \times 10^{-2}$
$5^2P \rightarrow 9^2S$	$1.505(16) \times 10^{-2}$	$1.5038(55) \times 10^{-2}$	$1.505(16) \times 10^{-2}$	$1.5038(55) \times 10^{-2}$	$1.505(16) \times 10^{-2}$	$1.5044(56) \times 10^{-2}$
$5^2P \rightarrow 10^2S$	$7.651(58) \times 10^{-3}$	$7.573(61) \times 10^{-3}$	$7.651(58) \times 10^{-3}$	$7.573(61) \times 10^{-3}$	$7.654(58) \times 10^{-3}$	$7.576(61) \times 10^{-3}$
$5^2P \rightarrow 11^2S$	$4.38(16) \times 10^{-3}$	$4.28(24) \times 10^{-3}$	$4.38(16) \times 10^{-3}$	$4.28(24) \times 10^{-3}$	$4.38(16) \times 10^{-3}$	$4.28(24) \times 10^{-3}$
$5^2P \rightarrow 12^2S$	$2.82(12) \times 10^{-3}$	$2.74(23) \times 10^{-3}$	$2.82(12) \times 10^{-3}$	$2.74(23) \times 10^{-3}$	$2.82(12) \times 10^{-3}$	$2.74(23) \times 10^{-3}$
$6^2S \rightarrow 6^2P$	2.154 30(48)	2.154 65(21)	2.154 48(46)	2.154 85(20)	2.156 10(42)	2.156 70(17)
$6^2S \rightarrow 7^2P$	$9.076(44) \times 10^{-2}$	$9.0837(70) \times 10^{-2}$	$9.073(45) \times 10^{-2}$	$9.0821(72) \times 10^{-2}$	$9.050(46) \times 10^{-2}$	$9.0684(72) \times 10^{-2}$
$6^2S \rightarrow 8^2P$	$2.210(14) \times 10^{-2}$	$2.2126(82) \times 10^{-2}$	$2.209(14) \times 10^{-2}$	$2.2121(82) \times 10^{-2}$	$2.206(14) \times 10^{-2}$	$2.2066(89) \times 10^{-2}$
$6^2S \rightarrow 9^2P$	$8.951(81) \times 10^{-3}$	$9.034(44) \times 10^{-3}$	$8.949(81) \times 10^{-3}$	$9.032(44) \times 10^{-3}$	$8.931(80) \times 10^{-3}$	$9.008(44) \times 10^{-3}$
$6^2S \rightarrow 10^2P$	$4.733(50) \times 10^{-3}$	$4.708(52) \times 10^{-3}$	$4.732(50) \times 10^{-3}$	$4.706(52) \times 10^{-3}$	$4.721(49) \times 10^{-3}$	$4.687(55) \times 10^{-3}$
$6^2P \rightarrow 7^2S$	$2.6067(72) \times 10^{-1}$	$2.6127(75) \times 10^{-1}$	$2.6092(72) \times 10^{-1}$	$2.6149(76) \times 10^{-1}$	$2.6326(74) \times 10^{-1}$	$2.6361(77) \times 10^{-1}$
$6^2P \rightarrow 8^2S$	$2.2665(68) \times 10^{-1}$	$2.2651(34) \times 10^{-1}$	$2.2643(68) \times 10^{-1}$	$2.2631(34) \times 10^{-1}$	$2.2415(68) \times 10^{-1}$	$2.2433(34) \times 10^{-1}$
$6^2P \rightarrow 9^2S$	$5.451(71) \times 10^{-2}$	$5.483(27) \times 10^{-2}$	$5.451(71) \times 10^{-2}$	$5.483(27) \times 10^{-2}$	$5.453(71) \times 10^{-2}$	$5.483(27) \times 10^{-2}$
$6^2P \rightarrow 10^2S$	$2.007(42) \times 10^{-2}$	$1.983(18) \times 10^{-2}$	$2.007(41) \times 10^{-2}$	$1.983(18) \times 10^{-2}$	$2.008(41) \times 10^{-2}$	$1.983(18) \times 10^{-2}$
$6^2P \rightarrow 11^2S$	$9.85(31) \times 10^{-3}$	$9.58(44) \times 10^{-3}$	$9.85(31) \times 10^{-3}$	$9.58(44) \times 10^{-3}$	$9.85(30) \times 10^{-3}$	$9.58(44) \times 10^{-3}$
$6^2P \rightarrow 12^2S$	$5.99(20) \times 10^{-3}$	$5.50(42) \times 10^{-3}$	$5.99(19) \times 10^{-3}$	$5.50(42) \times 10^{-3}$	$5.99(20) \times 10^{-3}$	$5.50(42) \times 10^{-3}$
$7^2S \rightarrow 7^2P$	$9.308(13) \times 10^{-1}$	$9.318(15) \times 10^{-1}$	$9.312(12) \times 10^{-1}$	$9.327(16) \times 10^{-1}$	$9.367(15) \times 10^{-1}$	$9.407(15) \times 10^{-1}$
$7^2S \rightarrow 8^2P$	$1.4463(53) \times 10^{-1}$	$1.4424(19) \times 10^{-1}$	$1.4460(55) \times 10^{-1}$	$1.4432(19) \times 10^{-1}$	$1.4434(62) \times 10^{-1}$	$1.4513(19) \times 10^{-1}$
$7^2S \rightarrow 9^2P$	$5.349(36) \times 10^{-2}$	$5.323(22) \times 10^{-2}$	$5.350(37) \times 10^{-2}$	$5.325(22) \times 10^{-2}$	$5.358(37) \times 10^{-2}$	$5.355(23) \times 10^{-2}$



TABLE VII. (Continued.)

Transition	$f_{ij}^L({}^{10}\text{B})$	$f_{ij}^V({}^{10}\text{B})$	$f_{ij}^L({}^{11}\text{B})$	$f_{ij}^V({}^{11}\text{B})$	$f_{ij}^L({}^{\infty}\text{B})$	$f_{ij}^V({}^{\infty}\text{B})$
$7^2S \rightarrow 10^2P$	$2.752(22) \times 10^{-2}$	$2.697(30) \times 10^{-2}$	$2.753(22) \times 10^{-2}$	$2.700(29) \times 10^{-2}$	$2.761(23) \times 10^{-2}$	$2.713(30) \times 10^{-2}$
$7^2P \rightarrow 9^2S$	$5.227(41) \times 10^{-1}$	$5.242(30) \times 10^{-1}$	$5.226(41) \times 10^{-1}$	$5.241(30) \times 10^{-1}$	$5.217(40) \times 10^{-1}$	$5.232(30) \times 10^{-1}$
$7^2P \rightarrow 10^2S$	$6.92(28) \times 10^{-2}$	$6.95(10) \times 10^{-2}$	$6.92(28) \times 10^{-2}$	$6.95(10) \times 10^{-2}$	$6.92(28) \times 10^{-2}$	$6.95(10) \times 10^{-2}$
$7^2P \rightarrow 11^2S$	$2.40(23) \times 10^{-2}$	$2.40(12) \times 10^{-2}$	$2.40(23) \times 10^{-2}$	$2.40(12) \times 10^{-2}$	$2.40(23) \times 10^{-2}$	$2.40(12) \times 10^{-2}$
$7^2P \rightarrow 12^2S$	$1.259(41) \times 10^{-2}$	$1.191(71) \times 10^{-2}$	$1.259(41) \times 10^{-2}$	$1.201(63) \times 10^{-2}$	$1.259(41) \times 10^{-2}$	$1.201(62) \times 10^{-2}$
$8^2S \rightarrow 7^2P$	1.349 5(70)	1.344 4(70)	1.347 9(70)	1.343 6(70)	1.332 0(69)	1.335 9(70)
$8^2S \rightarrow 8^2P$	$6.304(79) \times 10^{-2}$	$6.405(80) \times 10^{-2}$	$6.306(81) \times 10^{-2}$	$6.416(82) \times 10^{-2}$	$6.358(78) \times 10^{-2}$	$6.524(96) \times 10^{-2}$
$8^2S \rightarrow 9^2P$	$2.63(13) \times 10^{-2}$	$2.705(31) \times 10^{-2}$	$2.63(13) \times 10^{-2}$	$2.708(31) \times 10^{-2}$	$2.63(13) \times 10^{-2}$	$2.741(33) \times 10^{-2}$
$8^2S \rightarrow 10^2P$	$1.419(36) \times 10^{-2}$	$1.428(11) \times 10^{-2}$	$1.419(35) \times 10^{-2}$	$1.430(11) \times 10^{-2}$	$1.422(35) \times 10^{-2}$	$1.446(12) \times 10^{-2}$
$8^2P \rightarrow 10^2S$	$6.80(14) \times 10^{-1}$	$6.96(14) \times 10^{-1}$	$6.80(14) \times 10^{-1}$	$6.96(14) \times 10^{-1}$	$6.79(14) \times 10^{-1}$	$6.95(14) \times 10^{-1}$
$8^2P \rightarrow 11^2S$	$7.4(18) \times 10^{-2}$	$8.28(59) \times 10^{-2}$	$7.4(18) \times 10^{-2}$	$8.28(59) \times 10^{-2}$	$7.4(18) \times 10^{-2}$	$8.28(59) \times 10^{-2}$
$8^2P \rightarrow 12^2S$	$3.16(25) \times 10^{-2}$	$2.96(21) \times 10^{-2}$	$3.16(25) \times 10^{-2}$	$2.96(21) \times 10^{-2}$	$3.16(25) \times 10^{-2}$	$2.96(21) \times 10^{-2}$
$9^2S \rightarrow 8^2P$	2.712(19)	2.721(19)	2.712(19)	2.721(19)	2.707(19)	2.719(19)
$9^2S \rightarrow 9^2P$	$4.5(25) \times 10^{-4}$	$6.6(77) \times 10^{-5}$	$4.4(25) \times 10^{-4}$	$6.6(75) \times 10^{-5}$	$4.1(24) \times 10^{-4}$	$4.2(84) \times 10^{-5}$
$9^2S \rightarrow 10^2P$	$4.1(65) \times 10^{-4}$	$1.02(24) \times 10^{-3}$	$4.1(65) \times 10^{-4}$	$1.04(26) \times 10^{-3}$	$4.2(66) \times 10^{-4}$	$1.07(26) \times 10^{-3}$
$9^2P \rightarrow 11^2S$	$8.10(91) \times 10^{-1}$	$8.53(80) \times 10^{-1}$	$8.10(91) \times 10^{-1}$	$8.53(79) \times 10^{-1}$	$8.10(90) \times 10^{-1}$	$8.52(79) \times 10^{-1}$
$9^2P \rightarrow 12^2S$	$8.7(30) \times 10^{-2}$	$9.5(15) \times 10^{-2}$	$8.7(30) \times 10^{-2}$	$9.5(15) \times 10^{-2}$	$8.8(28) \times 10^{-2}$	$9.4(15) \times 10^{-2}$
$10^2S \rightarrow 9^2P$	3.305(80)	3.363(71)	3.296(87)	3.363(71)	3.293(87)	3.361(71)
$10^2S \rightarrow 10^2P$	$1.32(54) \times 10^{-2}$	$7.6(35) \times 10^{-3}$	$1.32(54) \times 10^{-2}$	$7.6(35) \times 10^{-3}$	$1.30(53) \times 10^{-2}$	$7.5(35) \times 10^{-3}$
$10^2P \rightarrow 12^2S$	$9.2(29) \times 10^{-1}$	1.14(34)	$9.2(29) \times 10^{-1}$	1.14(34)	$9.2(29) \times 10^{-1}$	1.14(34)
$11^2S \rightarrow 10^2P$	3.84(49)	3.75(43)	3.84(49)	3.75(43)	3.84(49)	3.74(43)

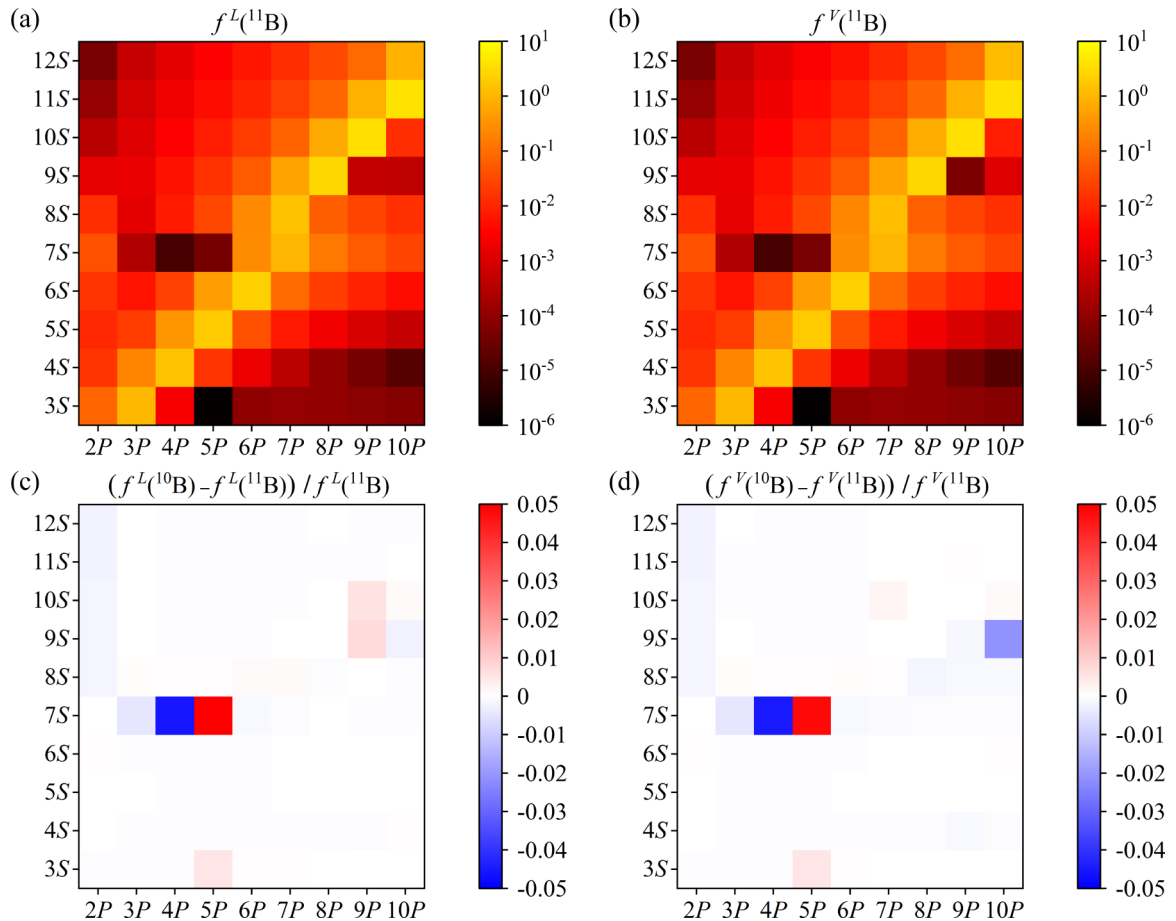


FIG. 1. Heat-map plot of the  ${}^{11}\text{B}$  oscillator strengths (a), (b), as well as of the relative isotopic shifts (c), (d) defined as  $[f({}^{10}\text{B}) - f({}^{11}\text{B})]/f({}^{11}\text{B})$ . Plots (a) and (c) on the left side of the figure show the results obtained using the length formalism, while those on the right side, (b) and (d), correspond to the velocity formalism.

TABLE VIII. List of transitions for which the magnitude of the relative isotopic shifts of the oscillator strength in the length ( $\text{RIS}^L$ ) and velocity ( $\text{RIS}^V$ ) gauges are most significant and exceed the value of  $2.5 \times 10^{-3}$ .

Transition	$\text{RIS}^L$	$\text{RIS}^V$
$5\ ^2P \rightarrow 7\ ^2S$	$5.08(10) \times 10^{-2}$	$4.805(33) \times 10^{-2}$
$4\ ^2P \rightarrow 7\ ^2S$	$-4.59(14) \times 10^{-2}$	$-4.498(73) \times 10^{-2}$
$9\ ^2S \rightarrow 9\ ^2P$	$1.75(89) \times 10^{-2}$	$1.31(25) \times 10^{-2}$
$3\ ^2S \rightarrow 5\ ^2P$	$5.562(61) \times 10^{-3}$	$5.452(46) \times 10^{-3}$
$3\ ^2P \rightarrow 7\ ^2S$	$-4.552(86) \times 10^{-3}$	$-4.624(63) \times 10^{-3}$

elements that involve the wave function largely described by such a configuration are very sensitive to the nuclear mass. We hope that one day the accuracy of future experimental data will be sufficient to resolve and confirm this peculiar behavior.

#### IV. SUMMARY

In this work, transitions between  $n\ ^2P$  ( $n = 2-10$ ) and  $n\ ^2S$  ( $n = 3-12$ ) states of the boron atom are studied. In the framework of the Rayleigh-Ritz variational method and expanding the wave function of each state with all-particle explicitly correlated Gaussian basis functions, we perform very accurate nonrelativistic calculations to determine the total energies and the corresponding wave functions of the considered states. The transition energies and the corresponding oscillator

strengths are calculated for the  $^2P \rightarrow ^2S$  and  $^2S \rightarrow ^2P$  transitions of the two stable boron isotopes,  $^{10}\text{B}$  and  $^{11}\text{B}$ , as well as for  $^{10}\text{B}$ . The calculated oscillator strengths show a certain pattern with the largest oscillator strength values appearing for the  $n\ ^2S \rightarrow n\ ^2P$  and  $n\ ^2P \rightarrow (n+1)\ ^2S$  transitions (i.e., the transitions between adjacent states) and much smaller values appearing for the other transitions, particularly those involving states with considerably different total energies. There is some interesting decrease of the oscillator strength for the  $4\ ^2P \rightarrow 7\ ^2S$  and  $5\ ^2P \rightarrow 7\ ^2S$  transitions that seems to be related to an anomaly of the configuration composition of the  $7\ ^2S$  state. Based on the oscillation-strength pattern, one can envision preparing a boron atom in a particular excited Rydberg state using an excitation cascade, e.g.,  $3\ ^2S \rightarrow 3\ ^2P$ ,  $3\ ^2P \rightarrow 4\ ^2S$ , ...

The data obtained in this work may be employed in modeling of light emission and absorption events involving boron isotopes in the laboratory and in the interstellar media. Such models usually require accurate values of the transition energies and the oscillator strengths which this work provides.

#### ACKNOWLEDGMENTS

This work has been supported by the National Science Foundation (Grant No. 1856702) and Nazarbayev University (faculty development Grant No. 021220FD3651). The authors acknowledge the use of computational resources provided by the University of Arizona (Puma and Ocelote clusters) and Nazarbayev University (Shabyt cluster).

- 
- [1] J. Rychlewski, *Explicitly Correlated Wave Functions in Chemistry and Physics: Theory and Applications*, Progress in Theoretical Chemistry and Physics (Kluwer, Dordrecht, 2003).
- [2] V. A. Yerokhin, V. Patkóš, and K. Pachucki, Atomic structure calculations of helium with correlated exponential functions, *Symmetry* **13**, 1246 (2021).
- [3] A. T. Bondy, D. C. Morton, and G. W. F. Drake, Two-photon decay rates in heliumlike ions: Finite-nuclear-mass effects, *Phys. Rev. A* **102**, 052807 (2020).
- [4] D. T. Aznabaev, A. K. Bekbaev, and V. I. Korobov, Nonrelativistic energy levels of helium atoms, *Phys. Rev. A* **98**, 012510 (2018).
- [5] V. Patkóš, V. A. Yerokhin, and K. Pachucki, Higher-order recoil corrections for singlet states of the helium atom, *Phys. Rev. A* **95**, 012508 (2017).
- [6] H. Nakatsuji and H. Nakashima, Free-complement local-Schrödinger-equation method for solving the Schrödinger equation of atoms and molecules: Basic theories and features, *J. Chem. Phys.* **142**, 084117 (2015).
- [7] C. Schwartz, Further computations of the He atom ground state, [arXiv:math-ph/0605018](https://arxiv.org/abs/math-ph/0605018) (2006).
- [8] L. M. Wang, Y. P. Zhang, D. Sun, and Z.-C. Yan, Nonrelativistic energies and fine-structure splittings for the Rydberg  $P$  states of lithium, *Phys. Rev. A* **102**, 052815 (2020).
- [9] L. M. Wang, C. Li, Z.-C. Yan, and G. W. F. Drake, Isotope shifts and transition frequencies for the  $S$  and  $P$  states of lithium: Bethe logarithms and second-order relativistic recoil, *Phys. Rev. A* **95**, 032504 (2017).
- [10] M. Puchalski and K. Pachucki, Ground-state hyperfine splitting in the  $\text{Be}^+$  ion, *Phys. Rev. A* **89**, 032510 (2014).
- [11] M. Puchalski and K. Pachucki, Quantum electrodynamics corrections to the  $2P$  fine splitting in Li, *Phys. Rev. Lett.* **113**, 073004 (2014).
- [12] M. Puchalski, K. Pachucki, and J. Komasa, Isotope shift in a beryllium atom, *Phys. Rev. A* **89**, 012506 (2014).
- [13] M. Puchalski and K. Pachucki, Applications of four-body exponentially correlated functions, *Phys. Rev. A* **81**, 052505 (2010).
- [14] K. Pachucki and J. Komasa, Nonrelativistic energy of tritium-containing hydrogen molecule isotopologues, *Mol. Phys.* **120**, e2040627 (2022).
- [15] M. Siłkowski, M. Zientkiewicz, and K. Pachucki, Accurate Born-Oppenheimer potentials for excited  $\Sigma^+$  states of the hydrogen molecule, in *New Electron Correlation Methods and their Applications, and Use of Atomic Orbitals with Exponential Asymptotes*, Advances in Quantum Chemistry, edited by M. Musial and P. E. Hoggan (Academic, New York, 2021), Chap. 12, Vol. 83, pp. 255–267.
- [16] M. Puchalski, J. Komasa, A. Spyszkiwicz, and K. Pachucki, Dissociation energy of molecular hydrogen isotopologues, *Phys. Rev. A* **100**, 020503(R) (2019).
- [17] V. S. Zotev and T. K. Rebane, Analytic evaluation of four-particle integrals with complex parameters, *Phys. Rev. A* **65**, 062501 (2002).
- [18] A. M. Frolov, Highly accurate calculation of the auxiliary functions of the fourth order and five-body integrals, *J. Phys. B: At., Mol. Opt. Phys.* **37**, 2103 (2004).

- [19] H. K. G. Büsse and A. Lüchow, Nonrelativistic energies for the Be atom: Double-linked hylleraas-CI calculation, *Int. J. Quantum Chem.* **66**, 241 (1998).
- [20] F. W. King, D. Quicker, and J. Langer, Compact wave functions for the beryllium isoelectronic series,  $\text{Li}^-$  to  $\text{Ne}^{6+}$ : A standard Hylleraas approach, *J. Chem. Phys.* **134**, 124114 (2011).
- [21] S. Bubin, M. Pavanello, W.-C. Tung, K. L. Sharkey, and L. Adamowicz, Born–Oppenheimer and Non-Born–Oppenheimer, atomic and molecular calculations with explicitly correlated Gaussians, *Chem. Rev.* **113**, 36 (2013).
- [22] J. Mitroy, S. Bubin, W. Horiuchi, Y. Suzuki, L. Adamowicz, W. Cencek, K. Szalewicz, J. Komasa, D. Blume, and K. Varga, Theory and application of explicitly correlated Gaussians, *Rev. Mod. Phys.* **85**, 693 (2013).
- [23] S. Nasiri, J. Liu, S. Bubin, M. Stanke, A. Kędzierski, and L. Adamowicz, Oscillator strengths and interstate transition energies involving  ${}^2S$  and  ${}^2P$  states of the Li atom, *At. Data Nucl. Data Tables* **149**, 101559 (2023).
- [24] S. Nasiri, T. Shomenov, S. Bubin, and L. Adamowicz, High-accuracy calculations of the lowest eleven Rydberg  ${}^2P$  states of Li atom, *J. Phys. B: At., Mol. Opt. Phys.* **54**, 085003 (2021).
- [25] S. Nasiri, L. Adamowicz, and S. Bubin, Benchmark calculations of the energy spectra and oscillator strengths of the beryllium atom, *J. Phys. Chem. Ref. Data* **50**, 043107 (2021).
- [26] S. Bubin and L. Adamowicz, Lowest  ${}^2S$  electronic excitations of the boron atom, *Phys. Rev. Lett.* **118**, 043001 (2017).
- [27] I. Hornyák, S. Nasiri, S. Bubin, and L. Adamowicz,  ${}^2S$  Rydberg spectrum of the boron atom, *Phys. Rev. A* **104**, 032809 (2021).
- [28] S. Nasiri, T. Shomenov, S. Bubin, and L. Adamowicz, Dissociation energy and the lowest vibrational transition in LiH without assuming the non-Born–Oppenheimer approximation, *Mol. Phys.* **120**, e2147105 (2022).
- [29] S. Nasiri, L. Adamowicz, and S. Bubin, Electron affinity of  $\text{LiH}^-$ , *Mol. Phys.* **120**, e2065375 (2022).
- [30] S. Nasiri, S. Bubin, and L. Adamowicz, Non-Born–Oppenheimer variational calculations of atoms and molecules with explicitly correlated Gaussian basis functions, in *Chemical Physics and Quantum Chemistry*, Advances in Quantum Chemistry, edited by K. Ruud and E. J. Brändas (Academic, New York, 2020), Chap. 5, Vol. 81, pp. 143–166.
- [31] S. Bubin and L. Adamowicz, Correlated-Gaussian calculations of the ground and low-lying excited states of the boron atom, *Phys. Rev. A* **83**, 022505 (2011).
- [32] B. Maaß, T. Hüther, K. König, J. Krämer, J. Krause, A. Lovato, P. Müller, K. Pachucki, M. Puchalski, R. Roth, R. Sánchez, F. Sommer, R. B. Wiringa, and W. Nörtershäuser, Nuclear charge radii of  ${}^{10,11}\text{B}$ , *Phys. Rev. Lett.* **122**, 182501 (2019).
- [33] M. Puchalski, J. Komasa, and K. Pachucki, Explicitly correlated wave function for a boron atom, *Phys. Rev. A* **92**, 062501 (2015).
- [34] K. Strasburger, Energy difference between the lowest doublet and quartet states of the boron atom, *Phys. Rev. A* **102**, 052806 (2020).
- [35] A. E. Kramida and A. N. Ryabtsev, A critical compilation of energy levels and spectral lines of neutral boron, *Phys. Scr.* **76**, 544 (2007).
- [36] H. Lundberg, Z. S. Li, and P. Jönsson, Experimental and theoretical investigations of radiative lifetimes in the s and d sequences of neutral boron, *Phys. Rev. A* **63**, 032505 (2001).
- [37] M. Wang, W. Huang, F. Kondev, G. Audi, and S. Naimi, The AME 2020 atomic mass evaluation (II). Tables, graphs and references, *Chin. Phys. C* **45**, 030003 (2021).
- [38] A. Hibbert, Atomic structure theory, in *Progress in Atomic Spectroscopy*, edited by W. Hanle and H. Kleinpoppen (Springer, Boston, 1978), pp. 1–69.
- [39] G. W. F. Drake, High precision calculations for Helium, in *Springer Handbook of Atomic, Molecular, and Optical Physics*, edited by G. W. F. Drake (Springer, New York, 2006), pp. 199–219.
- [40] C. Baxter, Center-of-mass motion of an  $N$ -particle atom or ion and the Thomas-Reiche-Kuhn sum rule, *Phys. Rev. A* **50**, 875 (1994).
- [41] B.-L. Zhou, J.-M. Zhu, and Z.-C. Yan, Generalized Thomas-Reiche-Kuhn sum rule, *Phys. Rev. A* **73**, 014501 (2006).
- [42] J. R. Fuhr and W. L. Wiese, Tables of atomic transition probabilities for beryllium and boron, *J. Phys. Chem. Ref. Data* **39**, 013101 (2010).
- [43] A. Kramida and K. Haris, Critically evaluated spectral data for singly ionized carbon (C ii), *Astrophys. J. Suppl. Ser.* **260**, 11 (2022).
- [44] G. Tachiev and C. F. Fischer, Breit-Pauli energy levels, lifetimes and transition data: boron-like spectra, *J. Phys. B: At., Mol. Opt. Phys.* **33**, 2419 (2000).
- [45] G. Tachiev and C. Froese Fischer, Breit-Pauli energy levels, lifetimes, and transition data: Beryllium-like spectra, *J. Phys. B: At., Mol. Opt. Phys.* **32**, 5805 (1999).
- [46] M. B. Ruiz, J. S. Sims, and B. Padhy, High-precision Hy-CI and E-Hy-CI studies of atomic and molecular properties, in *New Electron Correlation Methods and their Applications, and Use of Atomic Orbitals with Exponential Asymptotes*, Advances in Quantum Chemistry, edited by M. Musial and P. E. Hoggan (Academic, New York, 2021), Chap. 9, Vol. 83, pp. 171–208.
- [47] C. Chen, Energies, expectation values, fine structures and hyperfine structures of the ground state and excited states for boron, *Eur. Phys. J. D* **69**, 128 (2015).
- [48] C. Froese Fischer, S. Verdebout, M. Godefroid, P. Rynkun, P. Jönsson, and G. Gaigalas, Doublet-quartet energy separation in boron: A partitioned-correlation-function-interaction method, *Phys. Rev. A* **88**, 062506 (2013).
- [49] P. Seth, P. L. Ríos, and R. J. Needs, Quantum Monte Carlo study of the first-row atoms and ions, *J. Chem. Phys.* **134**, 084105 (2011).
- [50] C. X. Almora-Díaz and C. F. Bunge, Nonrelativistic CI calculations for  $\text{B}^+$ , B, and  $\text{B}^-$  ground states, *Int. J. Quantum Chem.* **110**, 2982 (2010).
- [51] I. Hornyák, L. Adamowicz, and S. Bubin, Ground and excited  ${}^1S$  states of the beryllium atom, *Phys. Rev. A* **100**, 032504 (2019).
- [52] J. Carlsson, P. Jönsson, L. Sturesson, and C. Froese Fischer, Lifetimes and transition probabilities of the boron atom calculated with the active-space multiconfiguration Hartree-Fock method, *Phys. Rev. A* **49**, 3426 (1994).
- [53] M. B. Ruiz, Configuration interaction study of the  ${}^3P$  ground and low-lying states of the boron anion. The boron electron affinity, in *State of The Art of Molecular Electronic Structure Computations: Correlation Methods, Basis Sets and More*, Ad-

- vances in Quantum Chemistry, edited by L. U. Ancarani and P. E. Hoggan (Academic, New York, 2019), Chap. 6, Vol. 79, pp. 135–153.
- [54] M. Stanke, A. Kędziorowski, S. Nasiri, L. Adamowicz, and S. Bubin, Fine structure of the  $^2P$  energy levels of singly ionized carbon (C II), *Phys. Rev. A* **108**, 012812 (2023).
- [55] E. Tiesinga, P. J. Mohr, D. B. Newell, and B. N. Taylor, CODATA recommended values of the fundamental physical constants: 2018, *Rev. Mod. Phys.* **93**, 025010 (2021).
- [56] K.-D. Wang, O. Zatsarinny, and K. Bartschat, Electron-impact excitation and ionization of atomic boron at low and intermediate energies, *Phys. Rev. A* **93**, 052715 (2016).
- [57] L. Argenti and R. Moccia, Autoionizing states of atomic boron, *Phys. Rev. A* **93**, 042503 (2016).
- [58] F. Weinhold, Calculation of upper and lower bounds to oscillator strengths, *J. Chem. Phys.* **54**, 1874 (1971).
- [59] F. Weinhold, *Upper and Lower Bounds to Quantum-Mechanical Properties* (Academic, New York, 1972), pp. 299–331.
- [60] P. Jennings and E. B. Wilson, Jr., Error bounds for expectation values, *J. Chem. Phys.* **45**, 1847 (1966).
- [61] J. R. Rumble, Jr., J. S. Sims, and D. R. Purdy, Upper and lower bounds for the oscillator strength of the  $X^1\Sigma_g^+ - C^1\Pi_u$  transition of the hydrogen molecule, *J. Phys. B: At. Mol. Phys.* **10**, 2553 (1977).
- [62] J. S. Sims and R. C. Whitten, Upper and lower bounds to atomic and molecular properties. I. Be-sequence oscillator strengths (Dipole-Length Formulation) for the  $1s^2 2s^2 \ ^1S - 1s^2 2s 2p \ ^1P$  Transition, *Phys. Rev. A* **8**, 2220 (1973).
- [63] J. S. Sims, B. Padhy, and M. B. R. Ruiz, Exponentially correlated hylleraas-configuration interaction studies of atomic systems. III. upper and lower bounds to He-sequence oscillator strengths for the resonance  $^1S \rightarrow ^1P$  transition, *Atoms* **11**, 107 (2023).